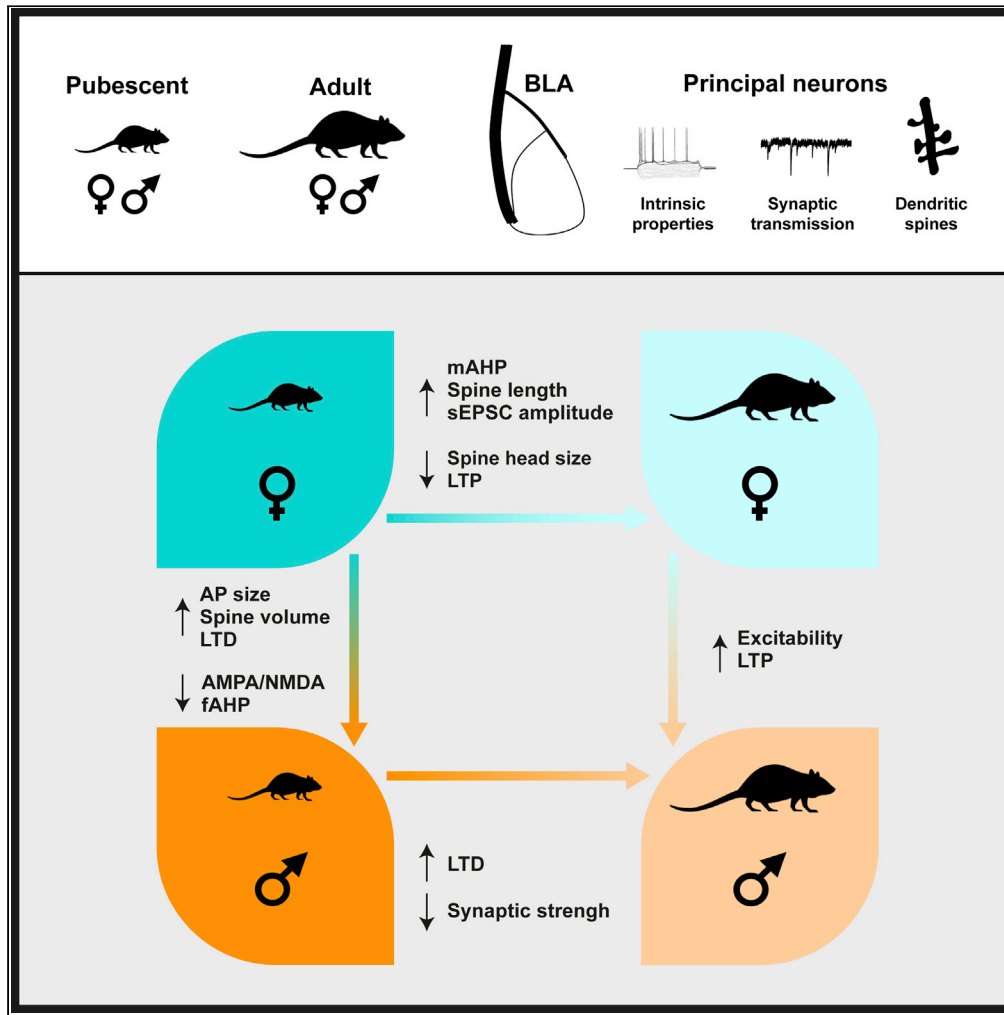**Article**

Sex-specific divergent maturational trajectories in the postnatal rat basolateral amygdala

Pauline Guily,
Olivier Lassalle,
Pascale Chavis,
Olivier J. Manzoni

olivier.manzoni@inserm.fr

Highlights

The BLA is immature at puberty and its development toward adulthood is sex-specific

At adulthood, neuronal excitability is lower in females than in males

The maturation of spine morphology is more pronounced in females

The developmental courses of LTP and LTD are sexually divergent

iScience

Article

Sex-specific divergent maturational trajectories in the postnatal rat basolateral amygdala

Pauline Guily,[1,2] Olivier Lassalle,[1,2] Pascale Chavis,[1,2] and Olivier J. Manzoni[1,2,3,*]

SUMMARY

In rodents and humans, the basolateral amygdala (BLA), essential for emotional behaviors, is profoundly reorganized during adolescence. We compared in both sexes the morphology, neuronal, and synaptic properties of BLA neurons in rats at puberty and adulthood. BLA neurons were more excitable in males than in females at adulthood. At pubescence, male action potentials were smaller and shorter than females' while fast afterhyperpolarizations were larger in males. During postnatal maturation, spine length increased and decreased in females and males, respectively, while there was a reduction in spine head size in females. Excitatory synaptic properties, estimated from stimuli-response relationships, spontaneous post-synaptic currents, and AMPA/NMDA ratio also displayed sex-specific maturational differences. Finally, the developmental courses of long-term potentiation and depression were sexually dimorphic. These data reveal divergent maturational trajectories in the BLA of male and female rats and suggest sex-specific substrates to the BLA linked behaviors at adolescence and adulthood.

INTRODUCTION

The basolateral amygdala (BLA), a limbic area massively connected to cortical and sub cortical structures, is at the interface of perception, emotion, and motor behaviors. Its role in the processing of fearful and rewarding stimuli, as well as emotional memory, is now well established (Bocchio et al., 2017; Janak and Tye, 2015; Phelps, 2004). A growing body of evidence indicates sex-differences in these functions (Cahill et al., 2004; Canli et al., 2002; Greiner et al., 2019; Gruene et al., 2015; Lebron-Milad and Milad, 2012). Moreover, the BLA is implicated in the etiology of neuropsychiatric diseases including post-traumatic stress disorder, depression, and anxiety (Daviu et al., 2019; Mahan and Ressler, 2012; Nestler et al., 2002), characterized by their higher prevalence in the female population (Christiansen and Berke, 2020; Kuehner, 2017; McLean et al., 2011).While the study of females' brains and sex differences in preclinical research have recently gained momentum (Shansky and Murphy, 2021), sex differences in the functions of the BLA have mostly been studied in pathological rodent models (Blume et al., 2019; Geary et al., 2021; Guadagno et al., 2020; Przybysz et al., 2021) and the physiological development of the female BLA remains partially understood.

At adolescence, neural networks are rearranged to allow the emergence of novel behaviors and the following transition to adult-specific circuits (Casey et al., 2008; Spear, 2000). Puberty is a particular time window of adolescent neurodevelopment, characterized by the arrival of sexual maturity and accompanied by a profound regulation of sex hormones (Schneider, 2013). Both adolescence and puberty are essential periods of postnatal brain maturation and are characterized by heightened susceptibility to mental disorders (Schneider, 2013). Studies also suggest that sex differences in depression prevalence emerge, or at least strengthen, during adolescence (Breslau et al., 2017). Additionally, there is consistent evidence indicating that the BLA activity is not mature at adolescence in humans (Scherf et al., 2013), and that puberty influences the maturation of the human amygdala (Bramen et al., 2011; Goddings et al., 2014). However, the magnitude of amygdala reorganization and possible sex differences during this period remain to be fully explored.

In adult rats, sex and estrus differences in excitatory and inhibitory inputs, as well as in the spine density of principal neurons residing in the lateral nucleus (LA) and the basal nucleus (BA) of the BLA have been reported (Blume et al., 2017). Long-term potentiation (LTP) of LA-BA synapses in both male and female juvenile rats has been described (Bender et al., 2017; Guadagno et al., 2020). LTP and long-term depression (LTD) are both sensitive to sexual hormones in the BLA (Bender et al., 2017; Krę;żel et al., 2001; Yang
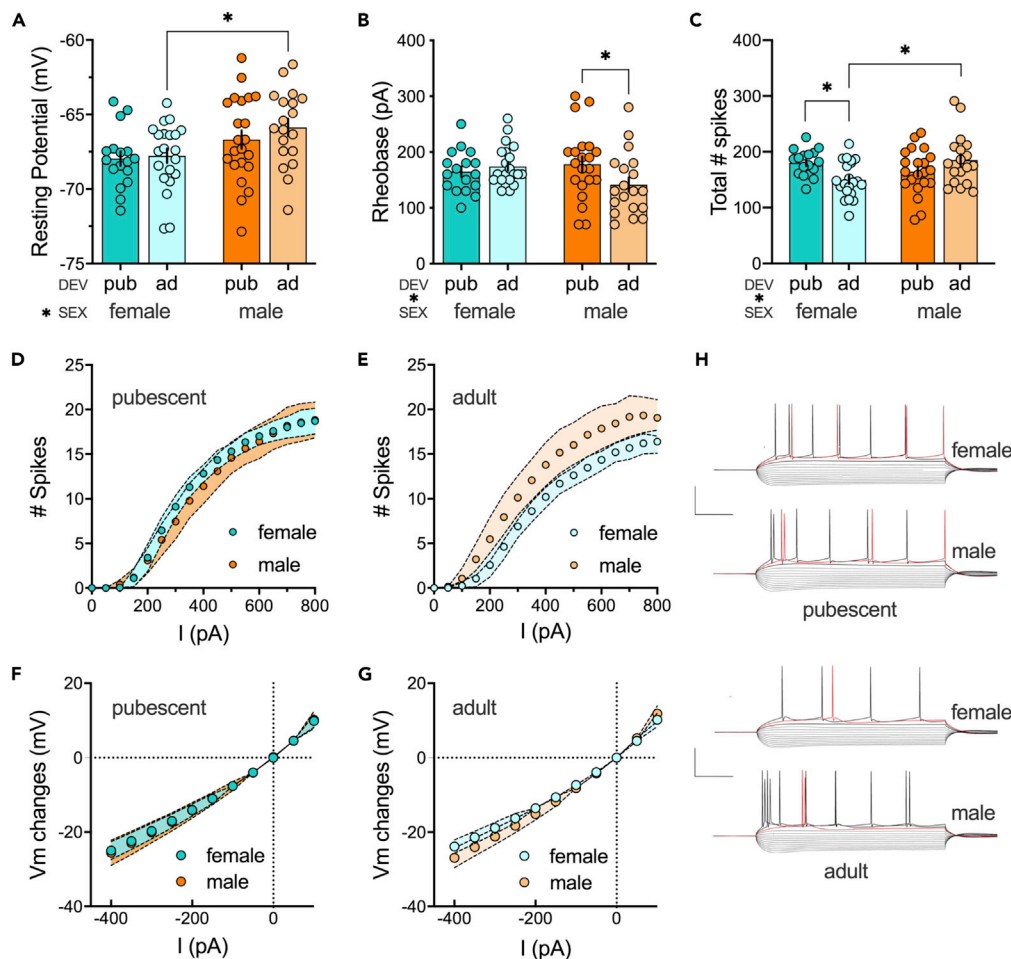
Figure 1. Sex-specific differences in intrinsic properties of rat BLA principal neurons emerge in adulthood

(A) Analysis of sex or development main effects and their interaction on the fAHP amplitude revealed that only sex had a significant effect (F (sex 1, 75) = 8.224, p = 0.0054). This effect was driven by significant sex-difference in adult rats, with hyperpolarized neurons in females compared with males (p = 0.0330).

(B) Progressive current injections in 10pA steps revealed that the minimal current required to trigger an action potential (i.e., rheobase) was influenced by sex and development interaction (F (sex X dev 1, 74) = 4.154, p = 0.0451). Post-hoc analysis revealed a higher rheobase in adult males compared with pubescent males (p = 0.0458) while females at different stage of maturation did not differ (p = 0.8036).

(C) Analysis of the total number of evoked action potentials in response to increasing depolarizing current revealed a significant sex × development interaction F (sex X dev 1, 73) = 9.085, pP = 0.0035). Adult females spiking less than both pubescent females (p = 0.0276) and adult males (p = 0.0078).

(D and E) Step by step analysis of the number of evoked action potentials in response to increasing depolarizing current was similar in pubescent rats of both sexes while neurons measured in adult males spiked more than of those of adult females.

(F and G) Current–voltage (I–V) curves from BLA pyramidal neurons were similar in pubescent and adult rats of both sexes.

(H) Typical membrane response to current steps of 50 pA from −400 pA to 250 pA in neurons of pubescent and adult rats of both sexes. Scale bar: 50 mV, 100 ms. Data are shown as mean ± SEM (A-C) or mean ±95% of CI (D-G). Pubescent: female, n = 17/10; male, n = 21–22/10–11. Adult: female, n = 21/12; male, n = 18–19/9–10. n = cells/rats. Data analyzed via two-way ANOVA followed by Šídák multiple comparison test (A–C). *p< 0.05. Color code: females, dark (pubescent) or light (adult) blue; males, dark (pubescent) or light (adult) orange.

et al., 2017), but little is known about sex-specific maturational trajectories of synaptic plasticity between puberty and adulthood. To our knowledge, no study to date has compared neuronal and synaptic proper-ties in the BLA during the pubertal period in both sexes. To address this gap in knowledge, we compared neuronal properties and excitatory transmission in the BLA of pubescent and adult rats of both sexes. Using *ex vivo* electrophysiological recordings in rat BLA slices, we report that excitatory neurons undergo com-plex sex-specific maturational sequence development. Some parameters such as intrinsic properties and

Table 1. Intrinsic properties data– Two-way ANOVAs

Measure (unit)	Condition		Value	Two-way ANOVA
RMP (mV)	F	Pub	−67.96 ± 0.4775 N = 17	F (sex x dev 1, 75) = 0.3157, p = 0.5759; **F (sex 1, 75) = 8.224 p = 0.0054**; F (dev 1, 75) = 0.8427 p = 0.3616
		Ad	−67.76 ± 0.4888 N = 21	
	M	Pub	−66.68 ± 0.6145 N = 22	
		Ad	−65.86 ± 0.5777 N = 19	
Rheobase (pA)	F	Pub	164.7 ± 9.120 N = 17	**F (sex x dev 1, 74) = 4.154, p = 0.0451**; F (sex 1, 74) = 0.7296, p = 0.3958; F (dev 1, 74) = 1.419, p = 0.2374
		Ad	174.3 ± 7.825 N = 21	
	M	Pub	178.1 ± 13.66 N = 21	
		Ad	141.6 ± 12.85 N = 19	
Total number of spikes	F	Pub	180.059 ± 5.717 N = 17	**F (sex x dev 1, 73) = 9.085, p = 0.0035**; F (sex 1, 73) = 1.368, p = 0.2460; F (dev 1, 73) = 0.3341 p = 0.5650
		Ad	149.714 ± 7.070 N = 21	
	M	Pub	164.476 ± 8.890 N = 21	
		Ad	185.055 ± 10.895 N = 18	

Values are mean ± SEM F: Female, M: Male, Pub: Pubescent, Ad: Adult. Bold characters represent statistics with significant p values.

action potential properties of neurons exhibit sex differences only at a specific time of development, whereas other parameters such as basic excitatory transmission and synaptic plasticity display different maturational profiles between male and female rats.

RESULTS

The aim of this study was 2-fold. First, we aimed to uncover potential sex differences at two key moments of development (pubescence and adulthood), and second, we compared maturational trajectories according to sex. Experiments were done in rats of both sexes at pubescent (female 33 <p< 38; male 41 <p< 56) and adult stages (at 90 <p< 120 for both sexes). All complementary statistics can be found in separated Tables.

Sex-specific differences in intrinsic properties of rat BLA principal neurons emerge in adulthood

Within the BLA, LA and BA principal neurons have distinct neuronal and synaptic properties (Blume et al., 2017). Thus, we purposely restrained this study to only one of these nuclei and chose the BA. Intrinsic properties are essential features of pyramidal neurons as well as key determinants of synaptic and network properties (Debanne and Poo, 2010). To compare intrinsic firing properties of principal neurons in our experimental groups, we performed patch-clamp recordings of BLA neurons in acute BLA slices obtained from pubescent and adult male or female rats and measured the membrane reaction profiles in response to a series of somatic current steps (Figure 1, Tables 1 and 2). Recording sites are reported in Figure S1.

At pubescence, all recorded BLA pyramidal neurons showed similar and superimposable I–V plots independent of sex (Figure 1F). Similarly, the resting membrane potential (Figure 1A) and the

Table 2. Intrinsic properties data - Multiple comparison tests

Sidak's multiple comparison test

Measure (unit)	F: Pub vs Ad	M: Pub vs Ad	Pub: M vs F	Ad: M vs F
RMP (mV)	p = 0.9622	p = 0.4941	p = 0.2089	**p = 0.0330**
Rheobase (pA)	p = 0.8036	**p = 0.0458**	p = 0.6543	p = 0.0809
Total # spikes	**p = 0.0276**	p = 0.1660	p = 0.3594	**p = 0.0078**

Values are mean ± SEM F: Female, M: Male, Pub: Pubescent, Ad: Adult. Bold characters represent statistics with significant p values.
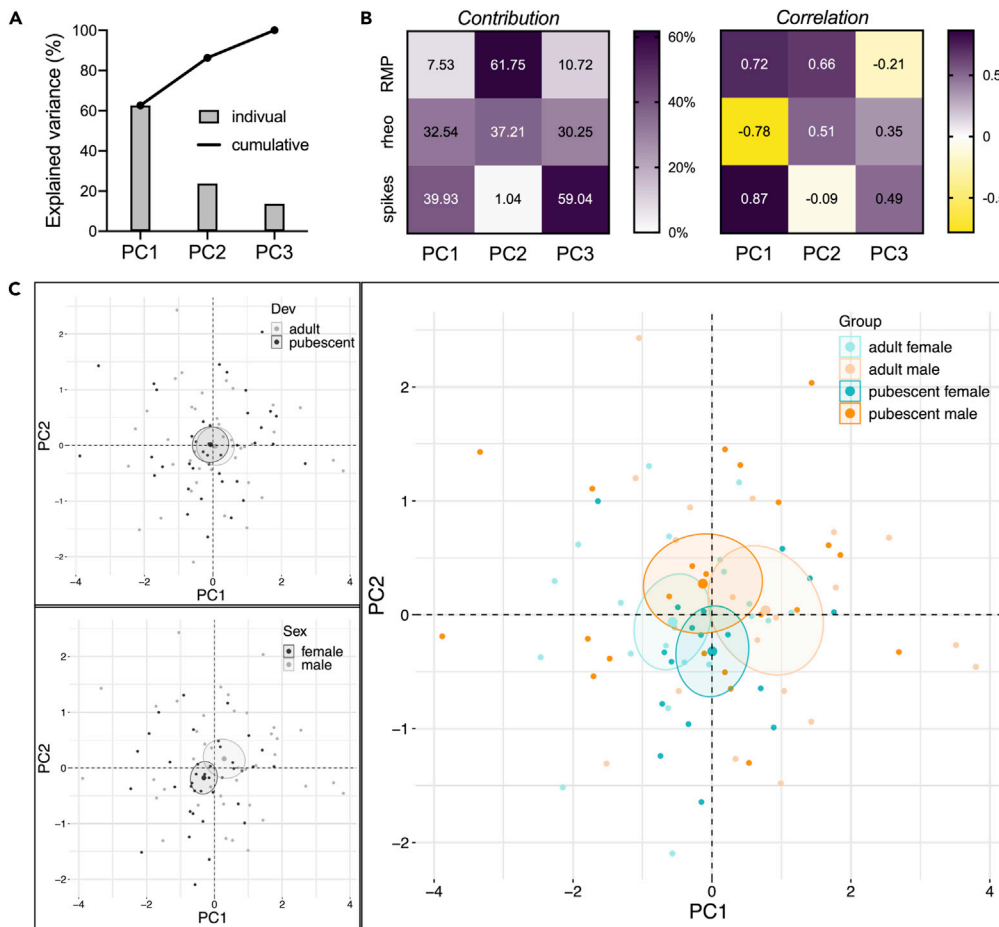
Figure 2. PCA of intrinsic properties show that sex is the principal contributor to the dataset variance

Data were analyzed via PCA with resting membrane potential (RMP), rheobase (rheo) and total number of spikes (spikes) as quantitative active variables and individual cells as individuals. Supplementary qualitive variables were development stage (dev, two modalities), sex (2 modalities) and group (4 modalities).

(A) Plotting the percentage of explained variance by each PC (histogram) reveals that most of the dataset's variance is explained by PC1 (62.6%), followed by PC2 (23.7%) and PC3 (13.7%). The cumulative percentage of explained is represented by black dots.

(B) Heatmaps representing the contribution (left) and correlation (right) of each variable with PCs 1, two and 3. (Left) Variables with the strongest contribution for a PC were used to build the PC (C) and individuals' coordinate on this axis provides information on the value taken by the individual for this variable. (Right) A positive correlation of a variable with a PC means that individuals that have high or low coordinates on the PC tend to have respectively high or low values for the variable. Conversely, a negative correlation means that individuals that have high coordinates on the PC tend to have low values for the variable or vice et versa.

(C) PCA graph of individuals was built with PC1 and PC2 which together explained more than 80% of the variance (see A). Small dots represent individuals colored according to their belonging to one the following qualitative supplementary variables: dev (top left), sex (bottom left), group (right). Bigger dots represent the barycenter of individuals (i.e., mean) for each category, surrounded by its 95% confidence ellipses (CE). PCA show that pubescents and adults CEs largely overlap (top left). In contrast, males and females CEs overlap only very partially (bottom left), in support of a large contribution of sex in the overall variance of intrinsic properties. Group analysis revealed that this effect is driven by a sex difference in adults (right). Cells obtained from adult males tend to spike more and have a lower rheobase (higher PC1 coordinates) than adult females (lower PC1 coordinates). Pubescent: female, n = 17/10; male, n = 21–22/10–11. Adult: female, n = 21/12; male, n = 18–19/9–10. n = cells/rats. Color code: females, dark (pubescent) or light (adult) blue; males, dark (pubescent) or light (adult) orange.

rheobase (Figure 1B) were similar within and between sex groups. In females but not males, the number of depolarization-driven spikes was larger at adolescence than adulthood (Figures 1C and 1D, Tables 1 and 2).
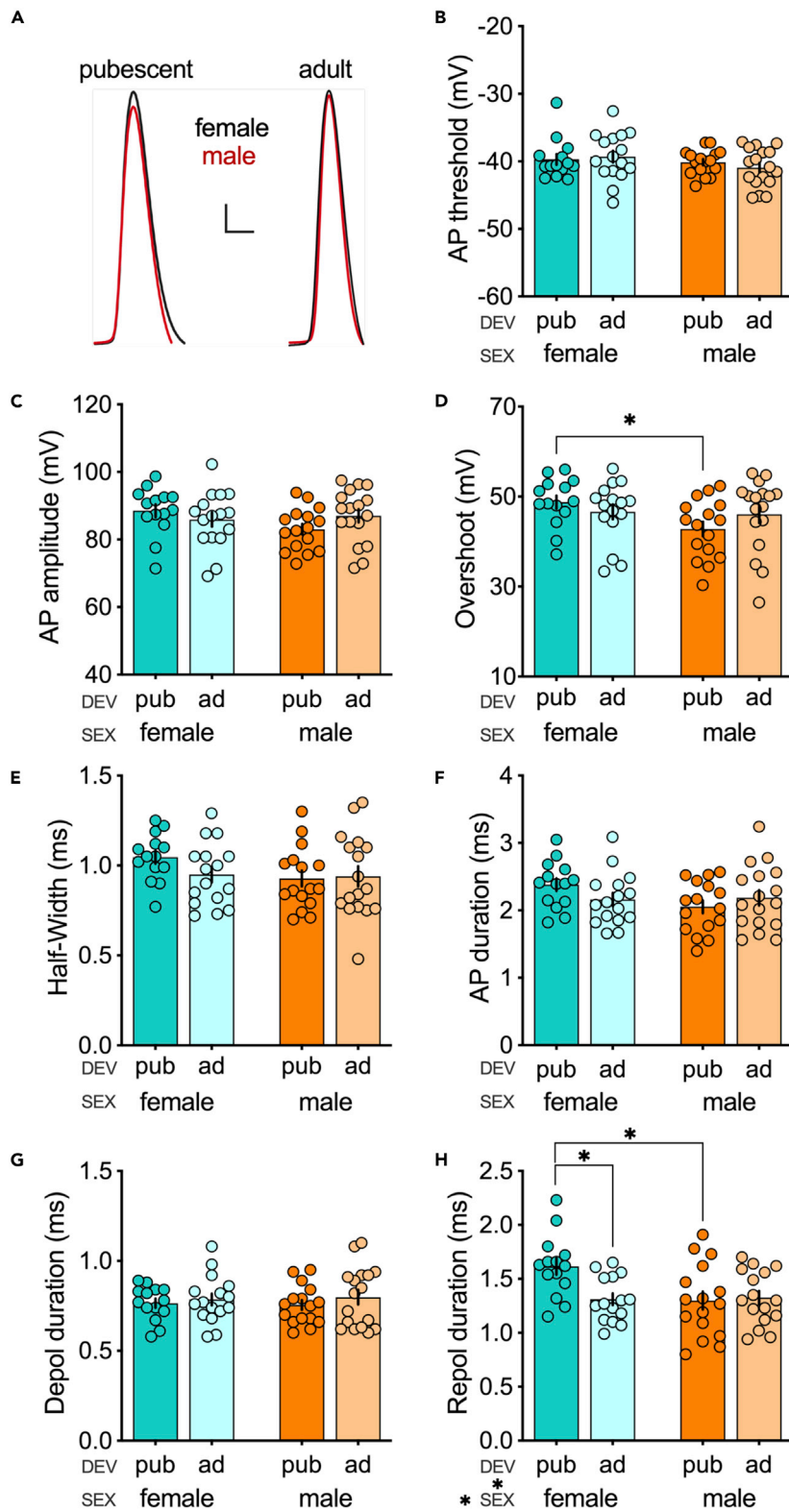
Figure 3. Action potential properties of principal neurons in the rat BLA

(A) Representative traces of the first spike elicited by a 10 pA current step injection in neurons of pubescent (right) and adult (left) rats. Male (red) and female (black) traces are superimposed for each developmental stage. Scale bar:10 mV, 1 ms.

(B) Action potential threshold did not vary between groups.

(C and D) Despite no difference in action potential amplitude (C), the overshoot was lower in pubescent males compared with females (D; p = 0.0392). This sex-difference was not found in adults (p = 0.9685). However, sex (F (sex 1, 59) = 3.573, p = 0.0637) and development (F (dev 1, 59) = 0.1067, p=0.7451) main effects, or sex × development interaction (F (sex X dev 1, 59) = 2.495, p = 0.1195), did not reach significance.

(E and F) Half-width (E) and action potential duration (F) did not vary between groups.

(G and H) Rise time was similar between each group (G). Conversely, the analysis of repolarization duration revealed a significant sex × development interaction (F (sex X dev 1, 56) = 6.918, p = 0.0110). Repolarization duration was shorter in pubescent males compared with females (p = 0.0025) whereas no difference was found between adult of both sexes (p = 0.9527). Pubescent females also presented a longer repolarization duration compared with adult females (p = 0.0152), whereas no difference was found between males of both ages (p = 0.6103). All data are shown as mean ± SEM Pubescent: female, n = 14/9; male, n = 16/10. Adult: female, n = 16/7; male = 17/10. n = cells/rats. Data analyzed via two-way ANOVA followed by Šídák multiple comparison test. *p< 0.05. Color code: females, dark (pubescent) or light (adult) blue; males, dark (pubescent) or light (adult) orange.

At adulthood, while I–V plots of males and females did not differ (Figure 1G), other differences emerged between sexes. Thus, the resting membrane potential (Figure 1A) of BLA pyramidal neurons significantly differed between sexes with male neurons being more depolarized than females. Furthermore, as estimated from the number of depolarization-driven spikes, adult males showed more action potentials in response to somatic current steps, compared with females (Figures 1C and 1E, Tables 1 and 2).

Further, Principal Component Analysis (PCA, Figure 2) with resting membrane potentials, rheobase and total number of spikes as quantitative variables, indicated that sex is the principal contributor to the dataset variance when all groups are considered. PCA also showed that the sex difference was the most pronounced during adulthood (Figure 2C).

Together these data show that sex-specific differences in intrinsic properties emerge at adulthood in BLA pyramidal neurons and that male BLA neurons display a higher excitability than female neurons at the same age.

Action potentials in BLA principal neurons diverge at pubescence

Changes in spike trains and excitability could partly be explained by changes in ion channel conductance which generate the different phases of action potentials (Hunsberger and Mynlieff, 2020; Matos et al., 2020; Zhang et al., 2020). To gain insight into this matter we next explored waveform properties of individual action potentials (Figure 3, Tables 3 and 4). Latency to first action potential was similar between groups (data not shown). While action potentials' threshold (Figure 3B), amplitude (Figure 3C), half-width (Figure 3E), duration (Figure 3F), and depolarization duration (Figure 3G) did not vary between our four groups, sex differences in other action potential properties were found in pubescent rats. Thus, at pubescence, action potentials' overshoot (Figure 3D) and repolarization duration (Figure 3H) were larger in females compared with males, supporting the existence of sex differences in the repolarization phase of pubescent rat. In females, there was a sex-specific maturation of repolarization duration that was shorter at adulthood (Figure 3H).

At adulthood, action potentials of BLA principal neurons displayed similar amplitude (Figure 3C), overshoot (Figure 3D), half-width (Figure 3E), and duration (Figure 3F).

Rather counter intuitively, these data suggest that in contrast to sex-differences in other intrinsic properties sex differences in action potential properties are only found at pubescence and disappear in adulthood in BLA principal neurons.

In continuity with the intrinsic properties (see Figures 1 and 2), PCA indicated that, again, sex is the principal contributor to the variance of this dataset (Figure 4).

The prolonged activation of calcium-dependent potassium channels (KCa) during the repolarization phase of action potentials leads to an afterhyperpolarization (AHP) potential below the action potential threshold.

Table 3. Action potential properties - two-way ANOVA

Measure (unit)	Condition		Value	two-way ANOVA
AP threshold (mV)	F	Pub	-39.69 ± 0.7882 N = 14	F (sex x dev 1, 59) = 0.7062, p = 0.404; F (sex 1, 59) = 2.087, p = 0.1539; F (dev 1, 59) = 0.06688, p = 0.7968
		Ad	-39.27 ± 0.8737 N = 16	
	M	Pub	-40.13 ± 0.4649 N = 16	
		Ad	-40.92 ± 0.6905 N = 17	
AP amplitude (mV)	F	Pub	88.53 ± 1.907 N = 14	F (sex x dev 1, 59) = 3.015 p = 0.0877; F (sex 1, 59) = 1.307 p = 0.2576; F (dev 1, 59) = 0.1274 p = 0.7224
		Ad	85.91 ± 2.103 N = 16	
	M	Pub	83.06 ± 1.557 N = 16	
		Ad	87.04 ± 1.954 N = 17	
AP overshoot (mV)	F	Pub	48.79 ± 1.455 N = 14	F (sex x dev 1, 59) = 2.495 p = 0.1195; F (sex 1, 59) = 3.573 p = 0.0637; F (dev 1, 59) = 0.1067 p = 0.7451
		Ad	46.63 ± 1.671 N = 16	
	M	Pub	42.80 ± 1.640 N = 16	
		Ad	46.09 ± 1.967 N = 17	
AP duration (ms)	F	Pub	2.381 ± 0.0932 N = 14	F (sex x dev 1, 59) = 3.016 p = 0.0876; F (sex 1, 59) = 2.166 p = 0.1464; F (dev 1, 59) = 0.1788 p = 0.6739
		Ad	2.161 ± 0.0950 N = 16	
	M	Pub	2.054 ± 0.0969 N = 16	
		Ad	2.188 ± 0.1151 N = 17	
Half-width (ms)	F	Pub	1.046 ± 0.03523 N = 14	F (sex x dev 1, 59) = 3.015 p = 0.0877; F (sex 1, 59) = 1.307 p = 0.2576; F (dev 1, 59) = 0.1274 p = 0.7224
		Ad	0.9506 ± 0.04366 N = 16	
	M	Pub	0.9281 ± 0.04343 N = 16	
		Ad	0.9406 ± 0.05602 N = 17	
Depolarisation time (ms)	F	Pub	0.7650 ± 0.0255 N = 14	F (sex x dev 1, 59) = 0.1180 p = 0.7325; F (sex 1, 59) = 0.001572 p = 0.9685; F (dev 1, 59) = 0.9410 p = 0.3360
		Ad	0.7856 ± 0.0329 N = 16	
	M	Pub	0.7550 ± 0.0270 N = 16	
		Ad	0.7982 ± 0.0406 N = 17	
Repolarisation time (ms)	F	Pub	1.616 ± 0.0772 N = 14	**F (sex x dev 1, 56) = 6.918 p = 0.0110;** **F (sex 1, 56) = 5.034 p = 0.0288;** F (dev 1, 56) = 1.986 p = 0.1643
		Ad	1.311 ± 0.0544 N = 15	
	M	Pub	1.299 ± 0.0840 N = 16	
		Ad	1.325 ± 0.0628 N = 17	
Rise time (ms)	F	Pub	0.2574 ± 0.01114 N = 14	F (sex x dev 1, 59) = 0.389 p = 0.5352; F (sex 1, 59) = 0.2930 p = 0.5903; F (dev 1, 59) = 1.275 p = 0.2635
		Ad	0.2349 ± 0.01320 N = 16	
	M	Pub	0.2424 ± 0.01230 N = 16	
		Ad	0.2359 ± 0.01387 N = 17	
Decay time (ms)	F	Pub	0.4764 ± 0.01627 N = 14	F (sex x dev 1, 59) = 3.146, p = 0.0813; F (sex 1, 59) = 2.939, p = 0.0917; F (dev 1, 59) = 0.8244, p = 0.3676
		Ad	0.4207 ± 0.01898 N = 16	
	M	Pub	0.4039 ± 0.02374 N = 16	
		Ad	0.4219 ± 0.02184 N = 17	

Values are mean $\pm$ SEM F: Female, M: Male, Pub: Pubescent, Ad: Adult. Bold characters represent statistics with significant p values.

The medium AHP (mAHP, Figure 5A), is tightly linked to neuronal excitability and sensitive to stress exposure in the BLA (Faber et al., 2001; Hetzel and Rosenkranz, 2014; Rau et al., 2015). Less is known about the fast AHP (fAHP, Figure 5A); however, it undergoes a profound maturation within the first postnatal month in the BLA (Ehrlich et al., 2012). The amplitudes of the fAHP and mAHP were measured in the first action potential recorded at the rheobase (Figure 5, Tables 5 and 6).

In every group, a large majority of neurons displayed a fAHP (Figure 5C). There was a significant effect of sex (p = 0.0204) and only a trend toward a significant effect of interaction between age and sex factors (p = 0.0590). These effects were driven by significantly greater fAHP amplitude in pubescent males compared with females. Note that the latter sex difference was no longer present in adults (Figure 5D).

Table 4. Action potential properties – Multiple comparison test

	Sidak's multiple comparison test			
Measure (unit)	F: Pub vs Ad	M: Pub vs Ad	Pub: M vs F	Ad: M vs F
AP threshold (mV)	p = 0.9036	p = 0.6735	p = 0.8964	p = 0.1950
AP amplitude (mV)	p = 0.5709	p = 0.2506	p = 0.1004	p = 0.8902
AP overshoot (mV)	p = 0.6286	p = 0.3145	**p = 0.0392**	p = 0.9685
AP duration (ms)	p = 0.2627	p = 0.5704	p = 0.0604	p = 0.9769
Half-width (ms)	p = 0.1601	p = 0.9846	p = 0.9727	p = 0.9846
Depol duration (ms)	p = 0.8891	p = 0.5706	p = 0.9727	p = 0.9525
Repol duration (ms)	**p = 0.0152**	p = 0.6103	**p = 0.0025**	p = 0.9527
Rise time (ms)	p = 0.4089	p = 0.9190	p = 0.6688	p = 0.9977
Decay time (ms)	p = 0.1335	p = 0.7814	**p = 0.0380**	p = 0.9988

Values are mean ± SEM F: Female, M: Male, Pub: Pubescent, Ad: Adult. Bold characters represent statistics with significant p values.

Further, there was a maturation of the mAHP in females, illustrated by a larger mAHP in adults compared with their pubescent counterparts (Figure 5E).

Synaptic properties in the BLA of pubescent and adult rats

Synaptic properties were compared and input-output curves constructed from the fEPSP amplitude versus increasing stimulation intensities at the BLA from brain slices of our four groups (Figure 6, Tables 7 and 8). Significant differences in stimulus-response relationship and maximal fEPSP amplitude were found between pubescent and adult males (Figures 6B and 6C). In females, the stimulus-response relationship did significantly vary between pubescents and adults (Figure 6A), however, the maximal fEPSP amplitudes did not (Figure 6C), despite a propensity toward larger fEPSP in pubescent females.

At excitatory synapses, the relative levels of AMPAR and NMDAR is a measure of synaptic integration and plasticity (Malinow and Malenka, 2002). We compared the ratio between AMPAR- and NMDAR-evoked EPSCs (AMPA/NMDA ratio) in adolescent and adult BLA neurons from rats of both sexes (Figure 7, Tables 9 and 10). This parameter significantly varied between males and females at pubescence (Figure 7B), males having a greater AMPA/NMDA ratio. In BLA slices of pubescent males, the bi-modal distribution of the data clearly shed light on two subgroups of neurons: one group displayed AMPA/NMDA ratio like females and the other exhibited AMPA/NMDA ratios higher than females (Figure 7C). In adult rats, the AMPA/NMDA ratio was similar across sexes (Figures 7B and 7D).

To extend our portrait of excitatory BLA synapses, AMPAR spontaneous EPSCs (sEPSCs) were isolated in BLA neurons voltage-clamped at −70 mV (Figure 8, Tables 11 and 12). Whereas the frequency of AMPAR sEPSCs remained invariable in females (Figure 8B), the distribution of sEPSC amplitudes was shifted toward lower values in adolescent female rats (Figure 8D). In contrast, both AMPA sEPSCs amplitude and frequency remained invariable in male littermates (Figures 8B and 8E).

Sex specific maturation of BLA neurons dendritic spines

Dendrites of BLA principal neurons are characterized by the presence of numerous spines which are the main contact of glutamatergic inputs (Brinley-Reed et al., 1995; Farb et al., 1992; Radley et al., 2007; Washburn and Moises, 1992). These spines are subject to intense maturational processes in the postnatal brain (Moyer and Zuo, 2018) and the BLA (Bosch and Ehrlich, 2015). Moreover, sex differences in spine density have also been reported in the adult BLA (Blume et al., 2017). Thus, to elucidate the sex-specific maturation of excitatory synapses in BLA principal neurons, we performed an *ex vivo* three-dimensional reconstruction of neurobiotin-filled BLA neurons (Figure 9, Tables 13, 14, 15, and 16).

Quantitative analysis of dendritic spine density and architecture revealed no change in the density of spines in our different groups (Figures 9A and 9B; all classes of spines were analyzed). Analyzing the total population of spines revealed a more pronounced maturation in females than males. Specifically, there was an augmentation in spine length (Figure 9C), paralleled by a reduction in spine head diameter (Figure 9D) and
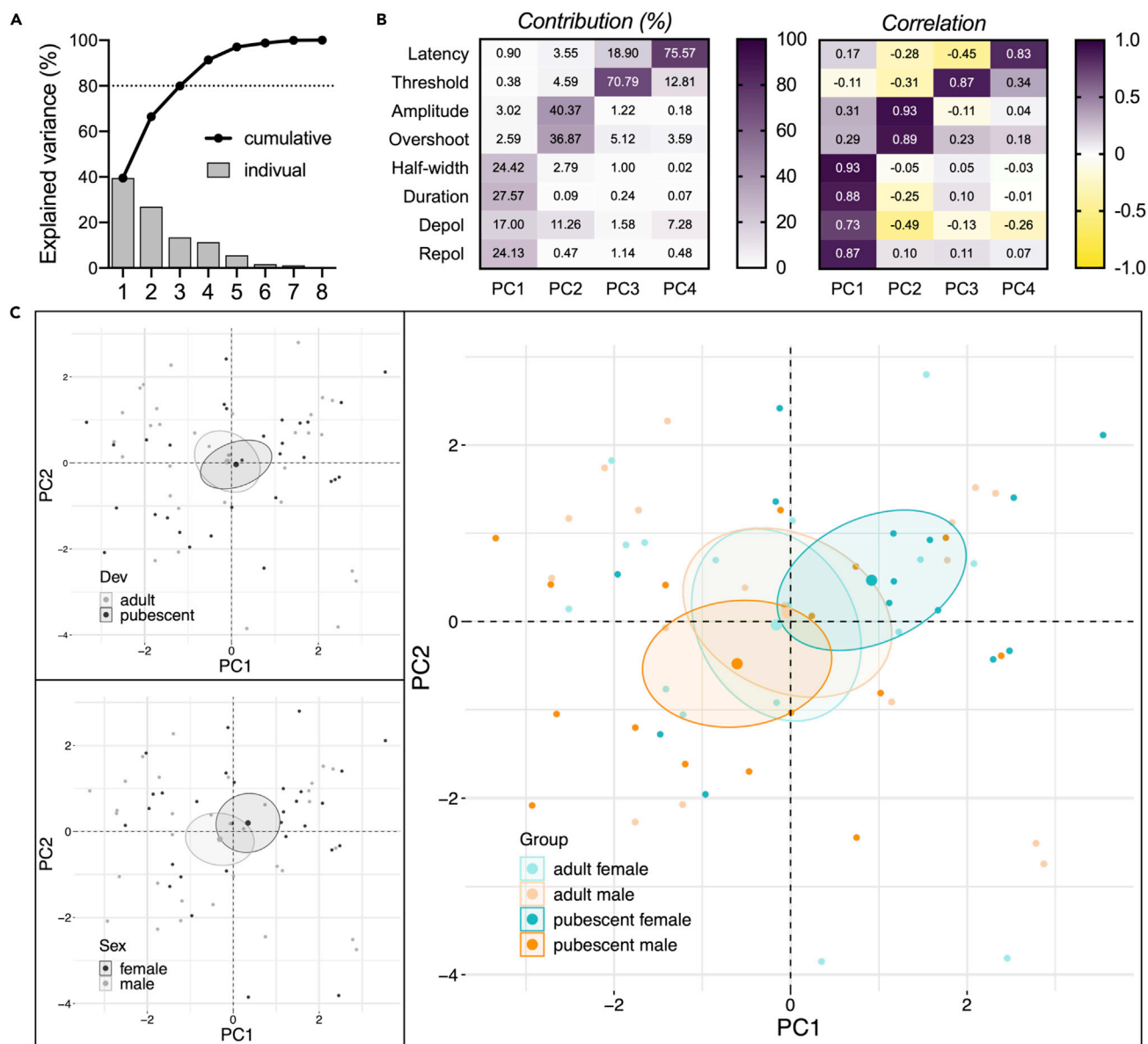
Figure 4. PCA of action potentials' properties suggest that sex is a major contributor to the dataset variance

Data were analyzed via PCA with action potential latency, threshold, amplitude, overshoot, half-width, duration, depolarization duration (depol) and repolarization duration (repol) as quantitative active variables and individual cells as individuals. Supplementary qualitive variables were development stage (dev, two modalities), sex (2 modalities) and group (4 modalities).

(A) Plotting the cumulative relative contribution of PCs against the variance reveals that most of the dataset's variance is explained by PC1 (39,5%), followed by PC2 (27,0%), PC3 (13,5%) and PC4 (11,4%).

(B) Heatmaps representing the contribution (left) and correlation (right) of each variable with PCs 1, 2, three and 4. (Left) Variables with the strongest contribution for a PC were used to build the PC (C) and individuals' coordinate on this axis provides information on the value taken by the individual for this variable. (Right) A positive correlation of a variable with a PC means that individuals that have high or low coordinates on the PC tend to have respectively high or low values for the variable. Conversely, a negative correlation means that individuals that have high coordinates on the PC tend to have low values for the variable or vice versa.

(C) PCA graph of individuals. Small dots represent individuals colored according to their belonging to one the following qualitative supplementary variables: dev (top left), sex (bottom left), group (right). Bigger dots represent the barycenter of individuals (i.e., mean) for each category, surrounded by its 95% confidence ellipses (CE). PCA show that pubescents and adults CEs largely overlap (top left). Males and females CEs overlap only partially (bottom left), in support of a substantial contribution of sex in the overall variance of action potentials' properties. Group analysis revealed the importance of a sex difference in pubescent in this effect (right). Cells obtained from pubescent females have longer and larger PAs (higher PC1 and PC2 coordinates, respectively) than pubescent males. Pubescent: female, n = 14/9; male, n = 16/10. Adult: female, n = 16/7; male = 17/10. n = cells/rats. Color code: females, dark (pubescent) or light (adult) blue; males, dark (pubescent) or light (adult) orange.
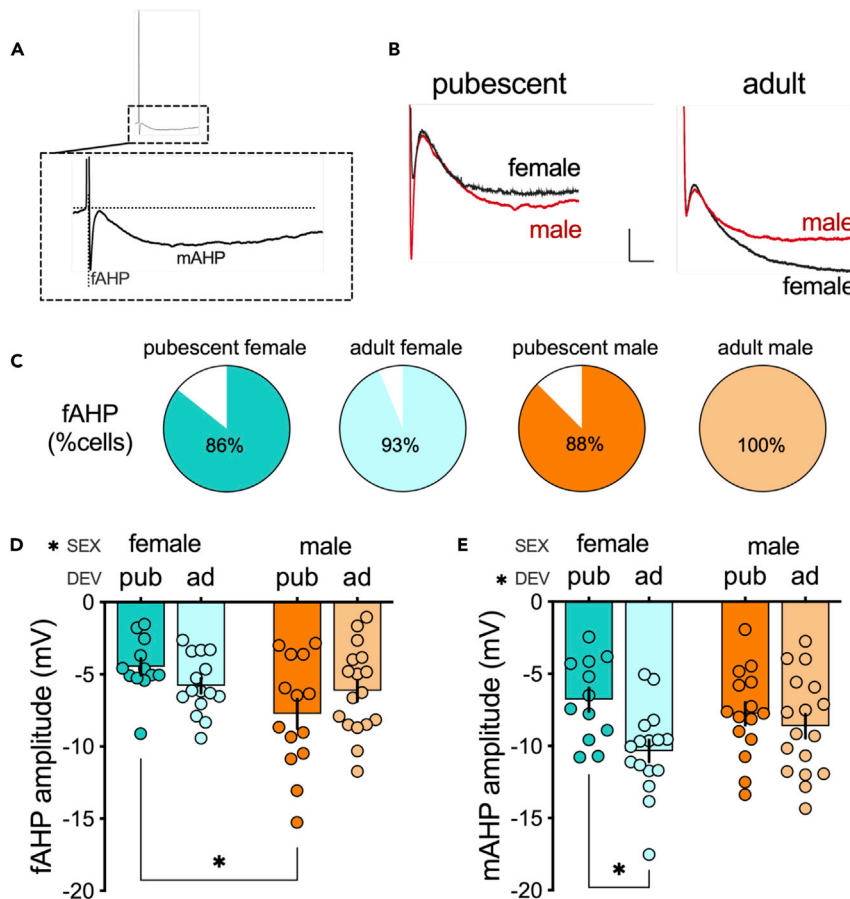
Figure 5. AHP profile of principal neurons in the rat BLA of pubescent and adult rat of both sexes

(A) Bottom: zoomed representation of the AHP of the action potential on the top. The fAHP is the local minimum directly following spike's repolarization within a couple of ms. The mAHP is a local minimum distinct from the fAHP and occurring 15–150 ms after the spike.

(B) Representative traces of the first spike's AHP elicited by a 10 pA current step injection in neurons of pubescent (left) and adult (right) rats. Male (red) and female (black) traces are superimposed for each development stage group. Scale bar: 2 mV, 20 ms.

(C) Proportion of cells with a first spike expressing a fAHP in pubescent (female, n = 12/14 cells, 86%; male, n = 14/16 cells, 88%) and adult (female, n = 15/16 cells, 93%; male, n = 17/17 cells, 100%) rats.

(D) Analysis of sex or development main effects and their interaction on the fAHP amplitude revealed that only sex had a significant effect (F (sex 1, 54) = 5.708, p = 0.0204). This effect was driven by significantly larger fAHPs in pubescent males compared with females (p = 0.0106). Pubescent: female, n = 12/9; male, n = 14/10. Adult: female, n = 1⁵/₈; male, n = 17/10. n = cells/rats.

(E) The mAHP amplitude was influenced by development (F (dev 1, 56) = 7.364, p = 0.0088). This main effect was driven by a significantly larger mAHP in adult females compared with pubescent females (p = 0.0084). Pubescent: female, n = 12/8; male, n = 15/9. Adult: female, n = 16/8; male, n = 17/10. n = cells/rats. All data are shown as mean ± SEM Data analyzed via two-way ANOVA followed by Šídák multiple comparison tests. *p< 0.05. Color code: females, dark (pubescent) or light (adult) blue; males, dark (pubescent) or light (adult) orange.

spine volume (Figure 9E) in adult females compared with pubescent females. In males, differences were restricted to a reduction in the spine length of adults compared with pubescent rats (Figure 9C). Selected sex differences manifested at pubescence: Spine head diameters and volumes were bigger in pubescent females than males (Figures 9D and 9E, respectively).

Theta-burst long-term potentiation follows a sex-specific maturational sequence in the rat BLA

Long-term potentiation (LTP) of excitatory synapses has been extensively studied in the BLA because of its role in fear learning and memory (Pape and Pare, 2010). While most studies measured LTP at sensory inputs

Table 5. AHP properties – two-way ANOVA

Measure (unit)	Condition		Value	Two-way ANOVA
fAHP amplitude (mV)	F	Pub	−4.473 ± 0.5803 N = 12	F (sex x dev 1, 54) = 3.720,
		Ad	−5.793 ± 0.5210 N = 15	p = 0.0590; F (sex 1, 54) = 5.708,
	M	Pub	−7.747 ± 1.034 N = 14	p = 0.0204; F (dev 1, 54) = 0.03558,
		Ad	−6.142 ± 0.7349 N = 17	p = 0.8511
Time to reach fAHP (ms)	F	Pub	0.8158 ± 0.05779 N = 12	F (sex x dev 1, 54) = 1.199,
		Ad	0.8450 ± 0.09886 N = 14	p = 0.2783; F (sex 1, 54) = 0.4541
	M	Pub	0.8644 ± 0.05324 N = 15	p = 0.5033; F (dev 1, 54) = 0.1553,
		Ad	0.7419 ± 0.05782 N = 17	p = 0.6951
mAHP amplitude (mV)	F	Pub	−6.797 ± 0.8187 N = 12	F (sex x dev 1, 56) = 2.763,
		Ad	−10.35 ± 0.7579 N = 16	p = 0.1020; F (sex 1, 56) = 0.2171,
	M	Pub	−7.769 ± 0.7879 N = 15	p = 0.6431; F (dev 1, 56) = 7.364,
		Ad	−8.624 ± 0.8335 N = 17	p = 0.0088
Time to reach mAHP (ms)	F	Pub	62.29 ± 5.277 N = 12	F (sex x dev 1, 56) = 0.0299,
		Ad	69.65 ± 4.681 N = 16	p = 0.863; F (sex 1, 56) = 1.933,
	M	Pub	53.29 ± 5.994 N = 15	p = 0.1700; F (dev 1, 56) = 2.108,
		Ad	62.64 ± 6.326 N = 17	p = 0.1521

Values are mean ± SEM F: Female, M: Male, Pub: Pubescent, Ad: Adult. Bold characters represent statistics with significant p values.

onto the LA, LTP at LA-BA synapses has also been reported in male and female rats at young ages (Bender et al., 2017; Guadagno et al., 2020). We elected to investigate LA-BA LTP in the BLA of male and female rats at our two age periods to test the hypothesis of a sexual dimorphism of BLA plasticity. We chose a mild induction protocol (theta burst stimulation, TBS) that allows detecting of altered LTP in rodent models of neuropsychiatric disorders (Iafrati et al., 2016; Labouesse et al., 2017; Manduca et al., 2017; Thomazeau et al., 2014). The LTP-induction protocol was applied to acute BLA slices obtained from our various rat groups during simultaneous recording of extracellular field EPSPs (Figure 10, Table 17).

In female BLA, while the TBS protocol effectively induced a lasting synaptic potentiation in slices obtained from pubescent rats, LTP was not induced by this protocol in slices prepared from adult rats (Figures 10A, 10C, and 10E). In contrast, TBS-LTP was consistently expressed in both pubescent and adult male rats (Figures 10B and 10D), albeit to a lesser level at the adult stage compared to adolescent counterpart. Indeed, when plotting the cumulative distribution of LTP percent, data distribution of adults was left shifted compared to pubescent rats, therefore indicating a reduction of TBS-LTP at adulthood (Figure 10F).

Long-term depression appears at adulthood in the BLA of male rats

Long-term depression (LTD) is a widespread form of synaptic plasticity (Malenka and Bear, 2004) also present in the rat BLA. Indeed, low frequency stimulation (1hz for 15 min, LFS) at LA-BA synapses reliably

Table 6. AHP properties - Multiple comparison tests

	Sidak's multiple comparison test			
Measure (unit)	F: Pub vs Ad	M: Pub vs Ad	Pub: M vs F	Ad: M vs F
fAHP amplitude (mV)	p = 0.4217	p = 0.2366	p = 0.0106	p = 0.9283
Time to reach fAHP (ms)	p = 0.8626	p = 0.4911	p = 0.9508	p = 0.3461
mAHP amplitude (mV)	p = 0.0084	p = 0.6895	p = 0.6688	p = 0.2206
Time to reach mAHP (ms)	p = 0.6242	p = 0.4182	p = 0.5067	p = 0.5990

Values are mean ± SEM F: Female, M: Male, Pub: Pubescent, Ad: Adult. Bold characters represent statistics with significant p values.
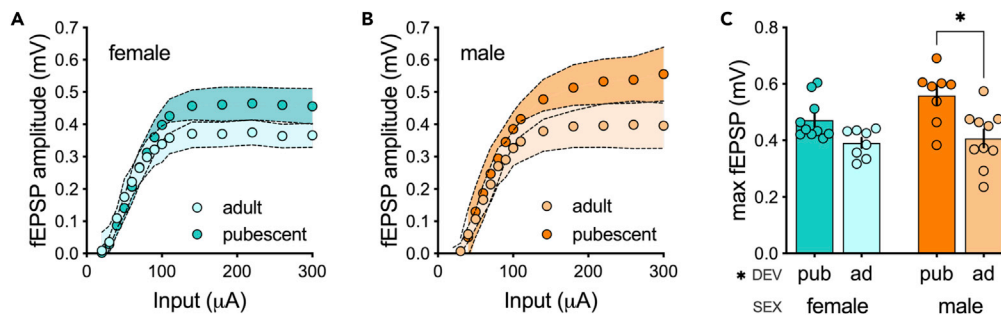
Figure 6. fEPSPs input-output profile
(A and B) Averaged fEPSP amplitude as a function of the stimulus intensity. There is a maturation of the input-output profile between pubescence and adulthood in both females (A) and males (B).
(C) Development influenced the maximum amplitude of fEPSPs, pubescent rats having larger fEPSPs than adults (F (dev 1, 32) = 17.59 p = 0.0002). This effect was driven by larger maximum fEPSPs in pubescents males compared with adults (p = 0.0010) while comparison between females of both developmental stages did not reach significance (p = 0.0943). n = individual rats, one slice per rat. Females: pubescent, n = 10; adult, n = 8. Males: pubescent, n = 10; adult, n = 8. n = cells/rats. Data are shown as mean ± CI (A-B) or ±SEM (C). Data analyzed via two-way ANOVA followed by Šídák multiple comparisons test (C). *p< 0.05. Color code: females, dark (pubescent) or light (adult) blue; males, dark (pubescent) or light (adult) orange.

induces LTD (Wang and Gean, 1999). Thus, we systematically compared LFS-LTD in the BLA of pubescent and adult rats of both sexes (Figure 11, Table 18). A 15-min, 1Hz stimulation in BLA slices obtained from females in both age groups induces a robust LTD (Figures 11A, 11C and 11E). This protocol likewise elicited LTD in slices obtained from adult males (Figures 11B, 11D and 11F). To our surprise, LFS-LTD could not be induced in response to this protocol in pubescent males (Figures 11B, 11D and 11F). Taken together, the results suggest a degree of sex specificity to the maturational profile of LFS-LTD and TBS-LTP.

DISCUSSION

Cross-sectional portrayal of the morphology and neuronal properties of BLA neurons in rats of both sexes revealed sex differences specific to adolescence and adulthood.

Sex differences in intrinsic properties of BLA neurons emerge at adulthood

We found that adult females had a higher rheobase, hyperpolarized membrane potential, and a lower propensity to trigger action potentials in response to depolarizing current steps than adult males. Consequently, principal neurons in the BLA of adult females are less excitable than those of adult males. Sex-differences in intrinsic properties of adult rats have already been described in other brain regions. Within the medial amygdala, a class of neurons exhibits lower spike frequency in response to depolarizing current in females than in males (Dalpian et al., 2019). In the medial nucleus of the central amygdala, Rouzer and Diaz also studied the sex-specific maturation of neurons intrinsic properties of adolescent and adult rats. While they found that males had lower AP thresholds than females suggesting more excitability in males, the quantification of spiking activity revealed that this was not directly translated in overall higher spiking activity in males than in females (Rouzer and Diaz, 2021). In the NAc core, medium spiny

Table 7. fEPSP input-output data - Two-way ANOV

Measure (unit)	Condition		Value	Two-way ANOVA
Maximum fEPSP amplitude (mV)	F	Pub	0.4715 ± 0.0229 N = 10	**F (sex x dev 1, 32) = 1.666, p = 0.2060; F (sex 1, 32) = 3.521, p = 0.0697; F (dev 1, 32) = 17.59, p = 0.0002**
		Ad	0.3911 ± 0.0176 N = 8	
	M	Pub	0.5593 ± 0.0338 N = 8	
		Ad	0.4073 ± 0.0316 N = 10	

Values are mean ± SEM F: Female, M: Male, Pub: Pubescent, Ad: Adult. Bold characters represent statistics with significant p values.

Table 8. fEPSP input-output data - Multiple comparison tests

	Sidak's multiple comparison test			
Measure (unit)	F: Pub vs Ad	M: Pub vs Ad	Pub: M vs F	Ad: M vs F
Maximum fEPSP amplitude (mV)	p = 0.0943	**p = 0.0010**	p = 0.0634	p = 0.8986

Values are mean ± SEM F: Female, M: Male, Pub: Pubescent, Ad: Adult. Bold characters represent statistics with significant p values.

neurons' intrinsic properties differ between males and females according to the estrous cycle phases (i.e., females are more excitable than males when in diestrus) (Proaño et al., 2018) and estradiol decrease the excitability of neurons from gonadectomized females (Proaño and Meitzen, 2020). Altogether, these
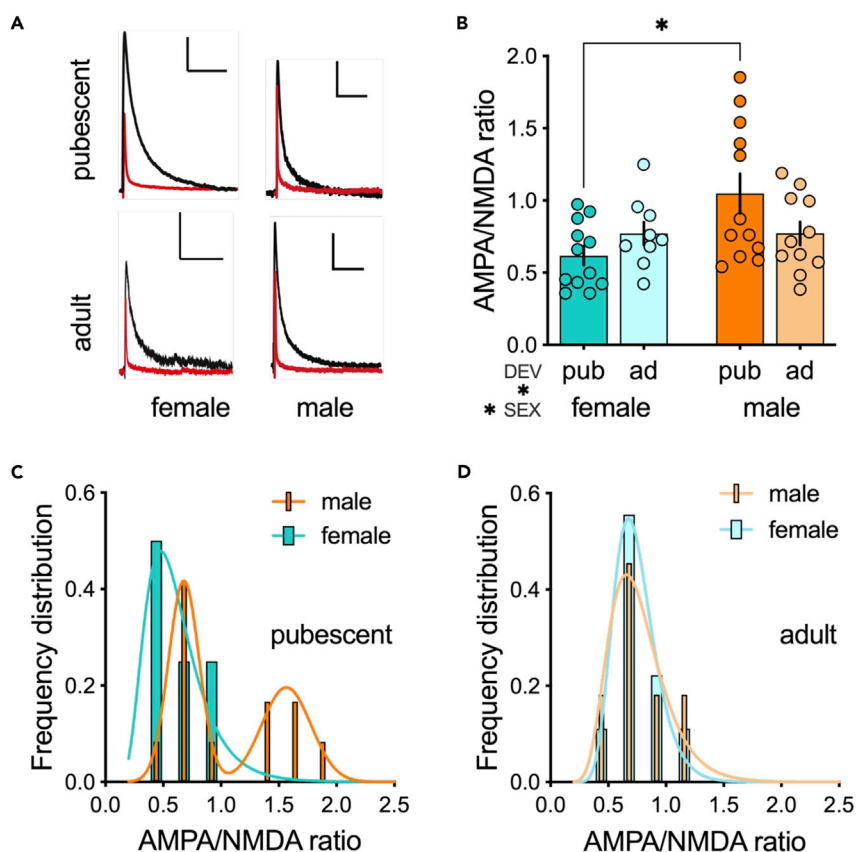

Figure 7. Sex-differences in AMPA/NMDA ratios disappear in adulthood

(A) Representative waveforms of AMPA EPSC evoked at +30mV in the presence of 50 μM APV (red) and NMDA EPSC obtained by digital subtraction of the AMPA component from the dual component EPSC evoked at +30mV (black). Scale bar: 50 pA, 500 ms.

(B) The analysis of AMPA/NMDA ratio revealed a significant sex × development interaction (F (sex X dev 1, 40) = 4.739 p = 0.0355). The AMPA/NMDA ratio of principal neurons was significantly higher in BLA slices obtained from pubescent males, as compared with those obtained from adult pubescent females (p = 0.0048). Conversely, no sex differences were found in adults (p> 0.999).

(C) Frequency distribution of AMPA/NMDA ratio reveals a subset of neurons from pubescent males with AMPA/NMDA ratio comparable to pubescent females, and another population of neurons with a greater AMPA/NMDA ratio. AMPA/NMDA ratio data from pubescent females were best fit by a single Gaussian (blue line), whereas data from pubescent males were best fit by the sum of two Gaussians (orange line), indicative of two populations.

(D) AMPA/NMDA ratio are distributed similarly between female and male adult rats. AMPA/NMDA ratio data of both groups best fit single gaussians. All data are shown as mean ± SEM Pubescent: female, n = 12/6; male, n = 12/9. Adult, female, n = 9/6; male, n = 11/7. n = cells/rats. Data were analyzed via two-way ANOVA followed by Šídák multiple comparisons test (B). *p< 0.05. Color code: females, dark (pubescent) or light (adult) blue; males, dark (pubescent) or light (adult) orange.

Table 9. AMPA/NMDA ratio data– two-way ANOVA

Measure (unit)	Condition		Value	Two-way ANOVA
AMPA/NMDA ratio	F	Pub	0.6181 ± 0.06533 N = 12	$F_{(sex \times dev\ 1, 40)} = 4.739$,
		Ad	0.7712 ± 0.07989 N = 9	$p = 0.0355$; $F_{(sex\ 1, 40)} = 4.769$,
	M	Pub	1.049 ± 0.1373 N = 12	$p = 0.0349$; $F_{(dev\ 1, 40)} = 0.3929$
		Ad	0.7719 ± 0.08110 N = 11	$p = 0.5343$

Values are mean ± SEM F: Female, M: Male, Pub: Pubescent, Ad: Adult. Bold characters represent statistics with significant p values.

results suggest that sex can profoundly influences principal neurons' excitability in multiple brain areas. Blood hormone levels were not assessed directly, and while one cannot totally exclude that this may participate to experimental variability, the current observation that sex differences are not visible at puberty at a time when the estrous cycle of females is not well established supports the instrumental role of gonadal hormones.

Stress exposure induces sex-divergent effects in the amygdala: BA neurons' firing rate augments in males and decreases in females (Blume et al., 2019). These changes have been attributed to stress-induced imbalance in excitation and inhibition (Blume et al., 2019; Mozhui et al., 2010; Rosenkranz et al., 2010; Zhang and Rosenkranz, 2012), and our results further suggest that initial sex differences in neuronal intrinsic excitability could participate in the divergent effect of stress seen in males and females.

Sex differences in action potentials emerge at pubescence

Pubescent males had shorter action potentials with faster repolarization compared with females. An early study reported that sex does not influence the maturation of action potential waveform during the first postnatal month (Ehrlich et al., 2012). However, Guadagno et al. observed that juvenile (PND22-PND29) males have shorter action potentials with slower depolarization rates compared with females (Guadagno et al., 2020). Here, we found sex differences reminiscent of those of pubescence (males still have shorter action potentials but faster repolarization). The current finding that the sex differences disappear in adults suggests a profound sex-specific maturation of action potentials from prepuberty through late adolescence.

Pubescent females displayed smaller fAHP compared with males. Changes in the expression of large conductance KCa (BKCa) may explain these dissimilarities (Sah and Louise Faber, 2002). In the LA, specific blockade of BKCa leads to smaller fAHPs and slower repolarizations of action potentials. Furthermore, stress exposure recapitulates these effects and is associated with a down-regulation of BKCa channels (Guo et al., 2012). Hence, a down-regulation of BKCa channels in pubescent females compared with males could participate in sex-differences in fAHP but also in repolarization. The parallel finding that the overshoot also differ between pubescent males and females is coherent with an implication of these channels, the overshoot being determined by the opening of BKCa which are both Ca and voltage sensitive and initiate the repolarization phase.

Unlike fAHP, mAHP amplitude was not influenced by sex. However, age did influence the mAHP, with larger mAHPs in adult females compared with pubescents. The mAHP results from the activation of apamine-sensitive small conductance KCa channels (Sah and Louise Faber, 2002). Our results are therefore consistent with that idea of sex-specific profiles of SK channels expression during maturation.

Mixed evidence implicates the mAHP in the modulation of intrinsic spiking frequency in BLA neurons (Chen and Lang, 2003; Faber and Sah, 2002; Power and Sah, 2008). Although multiple factors could explain these

Table 10. AMPA/NMDA ratio data - Multiple comparison tests

	Sidak's multiple comparison test			
Measure (unit)	F: Pub vs Ad	M: Pub vs Ad	Pub: M vs F	Ad: M vs F
AMPA/NMDA ratio	p = 0.4992	p = 0.0939	p = 0.0048	p> 0.9999

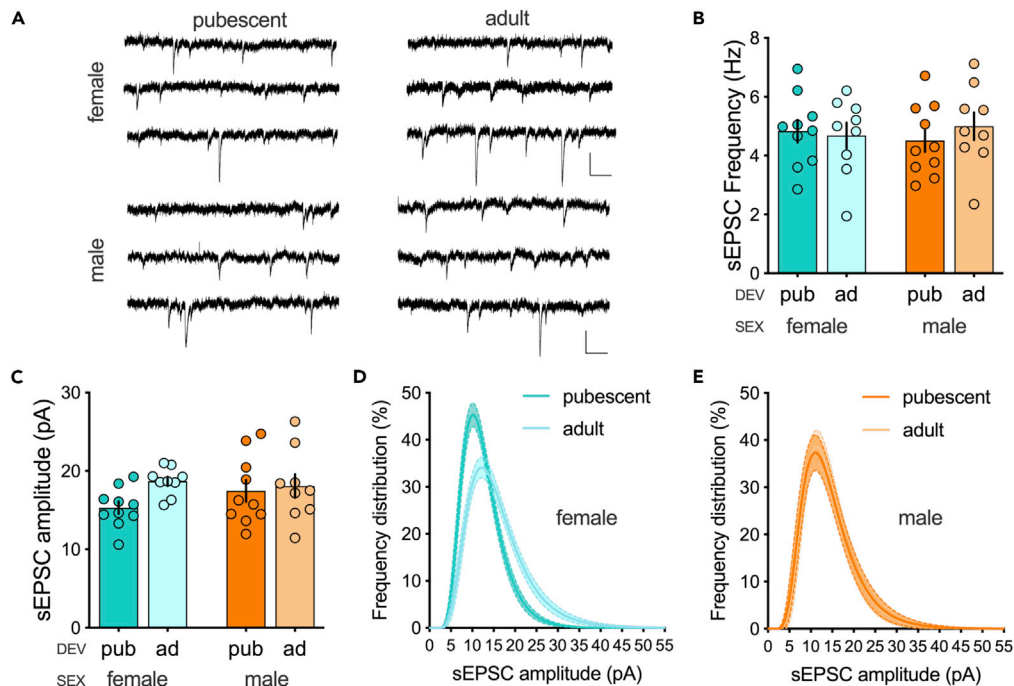Values are mean ± SEM F: Female, M: Male, Pub: Pubescent, Ad: Adult.

Figure 8. Amplitude distribution of sEPSCs is skewed toward larger amplitudes in adult females but not males BLA pyramidal neurons

(A) Representative traces of sEPSCs recorded at −70 mV in BLA pyramidal neurons. Scale bar: 20 pA, 100 ms.

(B) sEPSCs' mean frequency was similar for every group. There was no significant effect of development, sex, or their interaction, neither of any multiple comparison tests.

(C) sEPSCs' mean amplitude was similar for every group. There was no significant effect of development, sex, or their interaction, neither of any multiple comparison tests.

(D) Log-normal curve fit (±CI) of frequency distribution of individual sEPSCs' amplitude reveals a higher proportion of large size events in adult compared to pubescent female rats.

(E) Individual sEPSCs' amplitudes are distributed similarly in pubescent and adult males. Log-normal curve fit showing distributions' similar skewness between pubescent and adult males. All data are shown as mean ± SEM Females: pubescent, n = 10/8; adult, n = 9/7. Males: pubescent, n = 10/7; adult, 9/7. N = cells/rats. Data were analyzed via two-way ANOVA followed by Šídák multiple comparisons test (B and C), or two-way ANOVA of repeated measures followed by Tukey's multiple comparisons test for each sex (D-E). *p< 0.05. Color code: females, dark (pubescent) or light (adult) blue; males, dark (pubescent) or light (adult) orange.

discrepancies (the age of animals, *in vivo* versus *in vitro*, recording in LA or BA), smaller mAHP are consistently linked to an increased excitability. Furthermore, adolescent male rats that are responsive to restraint stress express higher spike frequency in both LA and BA neurons (Hetzel and Rosenkranz, 2014). While this increased excitability is accompanied by smaller mAHP in the LA, there was no effect on the mAHP in BA neurons. Thus, the mAHP is not constantly correlated with the spiking frequency in the BA. When we recorded BA neurons, the increased excitability seen in male adults compared females of the same age was not echoed by sex differences in the mAHP. Nevertheless, in pubescent, high spiking frequency and smaller mAHP were concomitant (Table 1).

Basic excitatory synaptic properties

We recently showed that the input profile and the release probability of excitatory synapses to prefrontal cortex (PFC) pyramidal neurons were consistent between pubescence and adulthood in both sexes (Bernabeu et al., 2020). In the BLA, the input-output curves built in pubescent rats reached higher maxima than in adults, in support of the idea that the BLA reaches maturity late in life. Pre-synaptic (e.g., release probability) or post-synaptic (e.g., receptor trafficking, AMPAR and NMDAR expression; Hwang and Lupica, 2020) maturation of the LA-BA synapses could explain the dissimilarities between pubescent and adult rats. In the present study, the AMPA/NMDA ratio in females was stable through development, and thus this mechanism is unlikely to account for the maturation of the input-profile in female rats. The AMPA/NMDA

Table 11. sEPSC properties data– two-way ANOVA

Measure (unit)	Condition		Value	Two-way ANOVA
sEPSC frequency (Hz)	M	Pub	4.514 ± 0.3845 N = 10	F (sex x dev 1, 34) = 0.5828,
		Ad	5.001 ± 0.4688 N = 9	p = 0.4505; F (sex 1, 34) = 1.483e-005,
	F	Pub	4.835 ± 0.3826 N = 10	p = 0.9969; F (dev 1, 34) = 0.1607,
		Ad	4.683 ± 0.4421 N = 9	p = 0.6910
sEPSC amplitude (pA)	M	Pub	17.46 ± 1.381 N = 10	F (sex x dev 1, 34) = 1.434,
		Ad	18.09 ± 1.511 N = 9	p = 0.2394; F (sex 1, 34) = 0.4593,
	F	Pub	15.32 ± 0.7851 N = 10	p = 0.5025; F (dev 1, 34) = 3.076,
		Ad	18.68 ± 0.5933 N = 9	p = 0.0885

Values are mean $\pm$ SEM F: Female, M: Male, Pub: Pubescent, Ad: Adult. Bold characters represent statistics with significant p values.

ratio of pubescent males was higher compared with females of the same age and this sex-difference was not found in adults. Interestingly, the distribution of AMPA/NMDA ratios was bimodal in pubescent but not adult males, perhaps an indication of a specific developmental signature in males. In contrast, previous work from our group conducted in the mice PFC demonstrated that AMPA/NMDA ratios remained stable between adolescence and adulthood (Iafrati et al., 2016). In the NAc (Kasanetz and Manzoni, 2009), AMPA/NMDA ratios are homogeneous in adolescent mice while they express a bimodal distribution in adults, contrary to what we observed in the BLA. Unfortunately, the studies did not include females. In any case, it is safe to conclude that the developmental trajectory of AMPA/NMDA ratios highly depends on the brain region.

The sex-specific maturation extended to sEPSCs whose amplitude augmented in adult females in keeping with the accompanying maturation of dendritic spines in this group (see below).

sEPSCs' properties remain overall comparable across sexes during maturation, suggesting that AMPA currents play a minor role in the high AMPA/NMDA ratios measured in pubescent males. In the BA of adult rats, mEPSCs' frequency was increased when females were in diestrus but comparable to males while in proestrus (Blume et al., 2017), leading to an overall increase in mEPSCs' frequency in females compared with males, while mEPSCs' amplitudes were similar. We did not observe such sex difference perhaps because of several methodological differences: our experiments were blind to the estrous cycle; we used coronal versus horizontal brain slices, we favored K^+ Gluconate internal medium over Cesium based solution, and we recorded spontaneous activity in the presence or absence of TTX.

Interestingly, Blume et al. correlated this sex-specific increase in frequency with an increase in spine density in females (independently of estrous cycle), while in our hands the lack of sex differences in sEPSCs was accompanied by stable dendritic spine density. Thus, the studies are divergent with one another, but coherent on their own, pointing to the possibility that somewhat different populations of neurons/dendrites were recorded/reconstructed. In support of this idea, one must note that Blume et al. discarded non pyramidal shaped neurons while we exploited all glutamatergic principal neurons, from stellate to pyramidal (See methods).

Dendritic spines

Our results replicate and extend upon previous morphological reconstructions of BLA principal neurons in male rats and mice showing that spine density remained stable between pubescence and adulthood (Bosch and Ehrlich, 2015; Ryan et al., 2016), by demonstrating that this remains the case in females.

Table 12. sEPSC properties data– Multiple comparison tests

Measure (unit)	Sidak's multiple comparison test			
	F: Pub vs Ad	M: Pub vs Ad	Pub: M vs F	Ad: M vs F
sEPSC frequency (Hz)	p = 0.9597	p = 0.6590	p = 0.8244	p = 0.8432
sEPSC amplitude (pA)	p = 0.0870	p = 0.9079	p = 0.3310	p = 0.9230

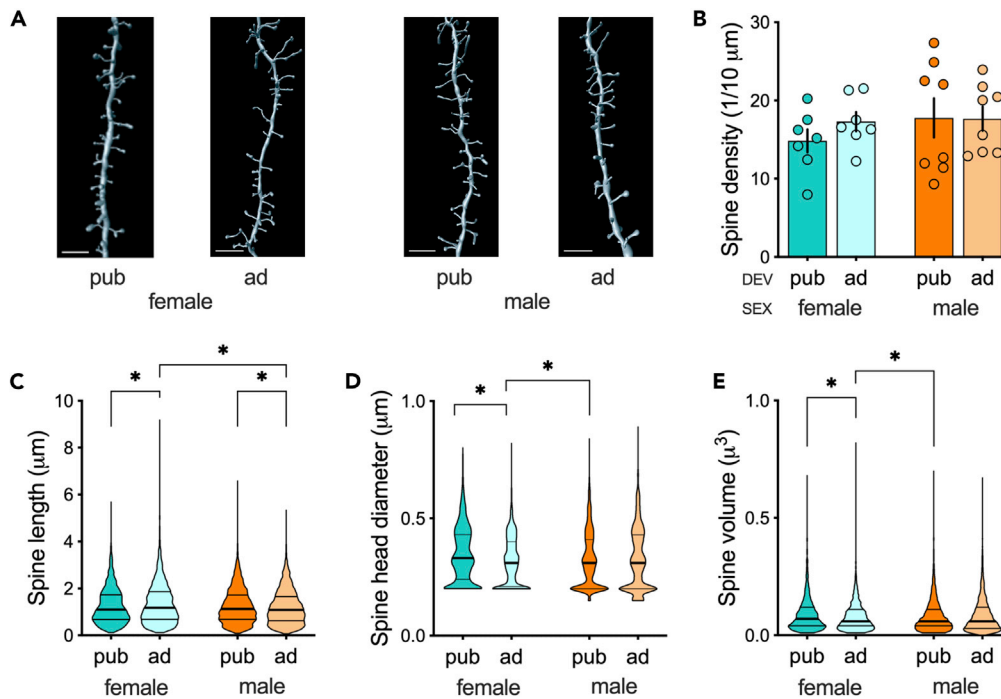Values are mean $\pm$ SEM F: Female, M: Male, Pub: Pubescent, Ad: Adult.

Figure 9. Sex-specific dendritic spine maturation of BLA principal neurons

(A) Representative 3D rendering of dendritic spines from neurobiotin filled principal neurons. Scale bar: 4 μm.

(B) Dendritic spine density was similar in all the groups. There was no significant effect of development, sex or their interaction, neither of any multiple comparison test. Females: pubescent, n = 7/7; adult, n = 7/4. Males: pubescent, n = 8/6; adult, n = 8/5. n = cells/rats.

(C) For neurons obtained from females, dendritic spines were shorter in pubescent compared with adult rats (p = 0.0061), whereas the opposite was found in males, with longer spines in pubescent compared with adult rats (p = 0.0018). Adult females also had longer spines compared with adult males (p< 0.0001). Females: pubescent, n = 2450; adult n = 3908. Males: pubescent, n = 4658; adult, n = 4639. n = spines.

(D) In females, spines' heads diameters were larger in pubescent compared with adult rats (p< 0.0001), whereas in males no significant development difference in spines' heads diameters was found (p> 0.9999). Pubescent females also had spines with larger heads compared with pubescent males (p< 0.0001). Females: pubescent, n = 2450; adult n = 3784. Males: pubescent, n = 4640; adult, n = 4585. n = spines.

(E) Spine volumes were bigger in pubescent females compared with both adult females and pubescent males. Females: pubescent, n = 2430; adult n = 3769. Males: pubescent, n = 4586; adult, n = 4540. n = spines. Data are shown as mean ± SEM (B) or violin plot with median (center), interquartile ranges (bounds), maxima and minima (C–E). Data were analyzed via two-way ANOVA followed by Šídák multiple comparisons test (B) or Kruskal-Wallis test followed by Dunn's multiple comparisons test (C–E). Color code: females, dark (pubescent) or light (adult) blue; males, dark (pubescent) or light (adult) orange.

Although we elected not to formally classify spines into the classical categories (thin, stubby, mushroom), the majority of spines identified in our rat groups were clearly thin as previously showed in the BLA (Zhang et al., 2019). Quantitative analysis of our data revealed a remodeling of dendritic spines after puberty,

Table 13. Dendritic spine density – two-way ANOVA

Measure (unit)	Condition		Value	Two-way ANOVA
Spine density (1/10μm)	M	Pub	17.77 ± 2.517 N = 8	F (sex x dev 1, 26) = 0.4965, p = 0.4873;
		Ad	17.67 ± 1.545 N = 8	F (sex 1, 26) = 0.8264, p = 0.3717; F (dev 1, 26) = 0.4236, p = 0.5209
	F	Pub	14.83 ± 1.476 N = 7	
		Ad	17.30 ± 1.236 N = 7	

Values are mean ± SEM F: Female, M: Male, Pub: Pubescent, Ad: Adult.

Table 14. Dendritic spine density – Multiple comparison tests

Measure (unit)	Sidak's multiple comparison test			
	F: Pub vs Ad	M: Pub vs Ad	Pub: M vs F	Ad: M vs F
Spine density (1/10μm)	p = 0.5929	p = 0.9990	p = 0.4587	p = 0.9870

Values are mean $\pm$ SEM F: Female, M: Male, Pub: Pubescent, Ad: Adult.

particularly in females. Principal neurons of pubescent females had shorter spine lengths, but larger spine head diameters and spine volumes. In the BLA, large spine head diameters do not correlate with large EPSC amplitude (Zhang et al., 2019), in agreement with the current lack of difference in sEPSCs amplitude in adults of both sexes (see above).

Sex influences the maturational profiles of LTP and LTD

The synaptic repertoire NMDAR is an important determinant of synaptic plasticity (Paoletti et al., 2013). Notably, in the BLA of young male rats (PND-17-24), GluN2A- and GluN2B-containing NMDAR subunits underlie LTP and LTD at auditory thalamic-LA pathway, respectively (Dalton et al., 2012). NMDAR activity or subunits mRNA expression can be modulated by gonadectomy in males (van den Buuse et al., 2017), estrous cycle in females (Picard et al., 2019), or sex (Damborsky and Winzer-Serhan, 2012; Qi et al., 2016). In the BLA, a recent study (Guadagno et al., 2020) did not report sex differences in NMDAR and AMPAR subunit protein levels in pre-pubertal rats, but showed a sex-dependent shift of protein levels in response to stress. While the developmental decrease of synaptic GluN2B-containing NMDARs is completed by the second postnatal week in certain areas such as the hippocampus and the NAc (Bellone and Nicoll, 2007; Chavis and Westbrook, 2001; Kasanetz and Manzoni, 2009; Mierau et al., 2004), it is delayed toward adulthood in the PFC (Iafrati et al., 2016), suggesting that NMDAR composition can fluctuate late in development. Altogether, these data suggest that the sex-dependent divergent maturational trajectories of LTP and LTD could be influenced by sex-specific maturation of NMDAR subtypes in the BLA.

TBS specifically failed to induce LTP in the BLA of adult females. Compelling evidence indicate sex-differences in LTP and learning (Gall et al., 2021). Several studies reported stronger LTP in males in the hippocampus of adult mice, while a five-paired theta burst akin to ours failed to induce LTP in female though triggered a robust LTP in males; conversely, a 10-paired TBS protocol induced LTP in both sexes, suggesting a higher threshold for LTP induction in females (Wang et al., 2018). Thus, in the CNS, sex differences in LTP are commonly observed and the BLA is no exception.

Table 15. Dendritic spine morphology data– Kruskal-Wallis tests

Measure (unit)	Condition		Value	Kruskal-Wallis test
Spine length (μm)	M	Pub	1.257 $\pm$ 0.01079 N = 4658	p< 0.0001
		Ad	1.206 $\pm$ 0.01067 N = 4639	
	F	Pub	1.261 $\pm$ 0.01514 N = 2450	
		Ad	1.365 $\pm$ 0.01450 N = 3908	
Spine head diameter (μm)	M	Pub	0.3264 $\pm$ 0.001784 N = 4640	p< 0.0001
		Ad	0.3284 $\pm$ 0.001928 N = 4585	
	F	Pub	0.3472 $\pm$ 0.002399 N = 2450	
		Ad	0.3213 $\pm$ 0.001678 N = 3784	
Spine volume (μm^3)	M	Pub	0.08388 $\pm$ 0.001039 N = 4586	p = 0.0002
		Ad	0.08596 $\pm$ 0.001131 N = 4540	
	F	Pub	0.08953 $\pm$ 0.001536 N = 2430	
		Ad	0.08053 $\pm$ 0.001105 N = 3769	

Values are mean $\pm$ SEM F: Female, M: Male, Pub: Pubescent, Ad: Adult. Bold characters represent statistics with significant p values.

Table 16. Dendritic spine morphology data– Multiple comparison tests

Measure (unit)	Dunn's multiple comparison test			
	F: Pub vs Ad	M: Pub vs Ad	Pub: M vs F	Ad: M vs F
Spine length (µm)	p = 0.0061	p = 0.0018	p> 0.9999	p< 0.0001
Spine head diameter (µm)	p< 0.0001	p> 0.9999	p< 0.0001	p> 0.9999
Spine volume (µm³)	p = 0.0002	p> 0.9999	p = 0.0018	p> 0.9999

Values are mean ± SEM F: Female, M: Male, Pub: Pubescent, Ad: Adult. Bold characters represent statistics with significant p values.
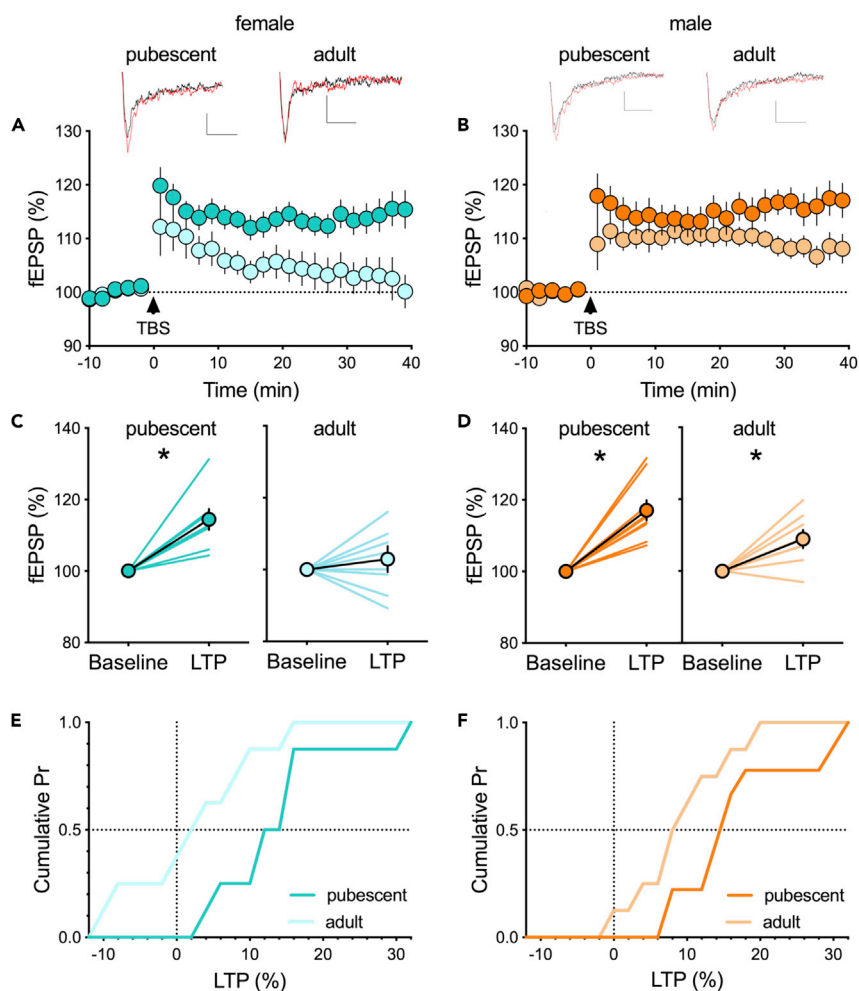

Figure 10. Age- and sex-dependent ablation of long-term potentiation (LTP) in the rat BLA

(A and B) Average time-courses of mean fEPSPs amplitude showing that theta-burst stimulation (TBS, indicated arrow) induced LTP at BLA synapses in pubescent females but not in adult females (A). In contrast, LTP was present in BLA slices obtained from both pubescent and adult male rats (B). Above: example traces, baseline (black) and 40 min post-stimulation (red). Scale bar: 0.1 mV, 10 ms.

(C and D) Individual experiments (simple line) and group average (circles) fEPSPs normalized amplitude before (baseline, −10 to 0 min) and after (LTP, 30–40 min) TBS showing the lack of LTP in adult females (C; pubescent, p = 0.0017; adult, p = 0.4797). In contrast, LTP was induced at both pubescent and adult males BLA synapses (D; pubescent, p = 0.0003; adult, p = 0.0090).

(E and F) Cumulative probability plot of percent LTP from individual experiments. Data are shown as mean ± SEM (A-D). Females: pubescent, n = 8; adult, n = 8. Males: pubescent, n = 9; adult, n = 8. n = individual rats, one slice per rat. Data were analyzed via paired t-test (C and D). *p< 0.05. Color code: females, dark (pubescent) or light (adult) blue; males, dark (pubescent) or light (adult) orange.

Table 17. TBS-LTP data

Measure (unit)	Condition		Value	Paired t test
TBS-LTP	F	Pub	114.5 ± 2.915 N = 8	**p = 0.0017**
Normalized fEPSP		Ad	102.4 ± 3.173 N = 8	p = 0.4797
0–10 min baseline (%) vs	M	Pub	117.0 ± 2.853 N = 9	**p = 0.0003**
30–40min post-tetanus (%)		Ad	109.2 ± 2.565 N = 8	**p = 0.0090**

Values are mean ± SEM F: Female, M: Male, Pub: Pubescent, Ad: Adult. Bold characters represent statistics with significant p values.
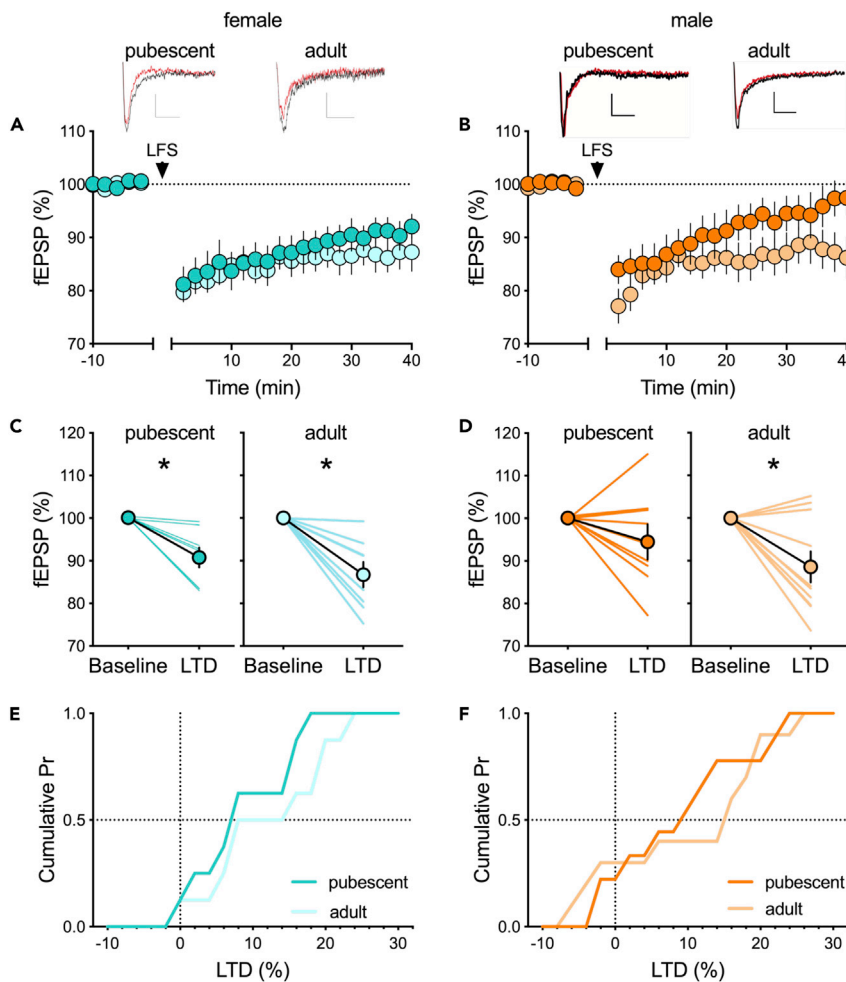
Figure 11. Long-term depression in the rat BLA

(A and B) Average time-courses of mean fEPSPs amplitude showing that low frequency stimulation, at 1Hz for 15 min (LFS, indicated arrow), induced LTD at BLA synapses in both pubescent and adult females (A). In contrast, LTD was present in BLA slices obtained from adult but not pubescent animals (B). Above: example traces, baseline (black) and 40 min post-stimulation (red). Scale bar: 0.1 mV, 10 ms.

(C and D) Individual experiments (simple line) and group average (circles) fEPSPs' normalized amplitude before (baseline, −10 to 0 min) and after (LTD, 30 to 40 min) LFS showing that LTD was present at both developmental stages in females (C; pubescent, p = 0.0139; adult, p = 0.0028). In contrast, LFS failed to induce a significant LTD in pubescent male slices, whereas it induced a significant LTD in adult male slices (D; pubescent, p = 0.2054; adult, p = 0.0118).

(E and F) Cumulative probability plot of percent LTD from individual experiments. Data are shown as mean ± SEM (A-D). Females: pubescent, n = 7; adult, n = 8. Males: pubescent, n = 10; adult, n = 9. n = individual rats, one slice per rat. Data were analyzed via paired t test (C and D). *p< 0.05. Color code: females, dark (pubescent) or light (adult) blue; males, dark (pubescent) or light (adult) orange.

Table 18. LFS-LTD data

Measure (unit)	Condition		Value	Paired t test
LFS-LTD	F	Pub	91.82 ± 2.432 N = 7	**p = 0.0139**
Normalized fEPSP		Ad	86.71 ± 2.968 N = 8	**p = 0.0028**
0–10 min baseline (%) vs	M	Pub	94.95 ± 3.676 N = 9	p = 0.2054
30–40min post-tetanus (%)		Ad	88.58 ± 3.635 N = 10	**p = 0.0118**

Values are mean ± SEM F: Female, M: Male, Pub: Pubescent, Ad: Adult. Bold characters represent statistics with significant p values.

Finally, LFS-LTD was present throughout maturation in females, but only emerged at adulthood in males. Interestingly, GABAergic inhibition is necessary to induce LFS-LTD in the BLA (Rammes et al., 2001). Even though GABAergic basic synaptic properties are mature at adolescence (Ehrlich et al., 2013), there is evidence showing that BLA circuits are less inhibited in adolescent pre-pubertal male rats (-PND40) than in adults (Selleck et al., 2018; Zhang and Rosenkranz, 2012). In addition, early stress exposure enhances LFS-LTD in the BLA (Danielewicz and Hess, 2014). In the hippocampus, stress exposure only enhances LTD in males in early adolescence and this is concomitant with sex-differences in both basal level of circulating corticosteroids and glucocorticoid receptors expression (Huang et al., 2012). Thus, potential lines of research to elucidate the mechanisms preventing LTD in pubescent males include GABAergic system and glucocorticoids.

Conclusion

In conclusion, these data illustrate how male and female rats follow divergent maturational trajectories and identify previously unreported sex-differences at adulthood. Taken together with previous work (Blume et al., 2017, 2019; Hetzel and Rosenkranz, 2014), this study highlights the complexity of the cellular substrates to the BLA linked sex-specific behaviors at adolescence and adulthood.

Both a bigger range of behavioral studies as well as extended characterizations of plasticity and synaptic functions in animals of both sexes in other brain regions are necessary to better understand how sex differences influence brain functions and behavior.

Limitations of the study

In our opinion, there are three main limitations to the present study. First, the trajectory of postnatal development was established by comparing pubescence to adulthood, two stages during which the brain is under the influence of sex hormones. Thus, the study could benefit from considering the juvenile period, a postnatal stage during which sex differences cannot be attributed to circulating sex hormones. This would clarify the contribution of sex hormones to the phenotypic differences reported here. Second, although the excitability and morphology of BLA principal neurons change during the estrous cycle (Blume et al., 2017), the hormonal status of females was not assessed in the current study. Third, although coactivation of inhibition and excitation is a basic functional principle in the CNS, we limited our *ex vivo* functional exploration to excitatory synapses. Recording inhibitory GABA synaptic inputs would allow us to assess the so-called balance of excitation and inhibition (E/I balance), a major gain mechanism that increases the precision and speed of neuronal response and increases the dynamic range of excitation.

STAR★METHODS

Detailed methods are provided in the online version of this paper and include the following:

- KEY RESOURCE TABLE
- RESOURCE AVAILABILITY
  - Lead contact
  - Materials availability
  - Data and code availability
- EXPERIMENTAL MODEL AND SUBJECT DETAILS
- METHOD DETAILS

- ○ Electrophysiology
- ○ Electrophysiological data analysis
- ○ Dendritic spines reconstruction and analysis
- ● QUANTIFICATION AND STATISTICAL ANALYSIS

AUTHOR CONTRIBUTIONS

P.G.: Conceptualization; Data curation; Formal analysis; Validation; Writing: review and editing. O.L.:Data curation; Formal analysis; Validation; Methodology. P.C.: Conceptualization; Methodology and editing. O.J.M.: Conceptualization; Supervision; Funding acquisition; Methodology; Writing: original draft, review and editing; Project administration.

DECLARATIONS OF INTERESTS

The authors declare no competing interests.

INCLUSION AND DIVERSITY

We worked to ensure sex balance in the selection of non-human subjects. One or more of the authors of this paper self-identifies as an underrepresented ethnic minority in science. One or more of the authors of this paper self-identifies as a member of the LGBTQ + community.

REFERENCES

Bara, A., Manduca, A., Bernabeu, A., Borsoi, M., Serviado, M., Lassalle, O., Murphy, M., Wager-Miller, J., Mackie, K., Pelissier-Alicot, A.-L., et al. (2018). Sex-dependent effects of in utero cannabinoid exposure on cortical function. eLife 7. https://doi.org/10.7554/eLife.36234.

Bellone, C., and Nicoll, R.A. (2007). Rapid bidirectional switching of synaptic NMDA receptors. Neuron 55, 779–785. https://doi.org/10.1016/j.neuron.2007.07.035.

Bender, R.A., Zhou, L., Vierk, R., Brandt, N., Keller, A., Gee, C.E., Schäfer, M.K.E., and Rune, G.M. (2017). Sex-dependent regulation of aromatase-mediated synaptic plasticity in the basolateral amygdala. J. Neurosci. 37, 1532–1545. https://doi.org/10.1523/JNEUROSCI.1532-16.2016.

Bernabeu, A., Bara, A., Manduca, A., Borsoi, M., Lassalle, O., Pelissier-Alicot, A.-L., and Manzoni, O.J. (2020). Sex-specific maturational trajectory of endocannabinoid plasticity in the rat prefrontal cortex (preprint). Neurosciences. https://doi.org/10.1101/2020.10.09.332965.

Blume, S.R., Freedberg, M., Vantrease, J.E., Chan, R., Padival, M., Record, M.J., DeJoseph,

M.R., Urban, J.H., and Rosenkranz, J.A. (2017). Sex- and estrus-dependent differences in rat basolateral amygdala. J. Neurosci. 37, 10567–10586. https://doi.org/10.1523/JNEUROSCI.0758-17.2017.

Blume, S.R., Padival, M., Urban, J.H., and Rosenkranz, J.A. (2019). Disruptive effects of repeated stress on basolateral amygdala neurons and fear behavior across the estrous cycle in rats. Sci. Rep. 9, 12292. https://doi.org/10.1038/s41598-019-48683-3.

Bocchio, M., Nabavi, S., and Capogna, M. (2017). Synaptic plasticity, engrams, and network oscillations in amygdala circuits for storage and retrieval of emotional memories. Neuron 94, 731–743. https://doi.org/10.1016/j.neuron.2017.03.022.

Borsoi, M., Manduca, A., Bara, A., Lassalle, O., Pelissier-Alicot, A.-L., and Manzoni, O.J. (2019). Sex differences in the behavioral and synaptic consequences of a single in vivo exposure to the synthetic cannabimimetic WIN55,212-2 at puberty and adulthood. Front. Behav.Neurosci. 13, 23. https://doi.org/10.3389/fnbeh.2019.00023.

Bosch, D., and Ehrlich, I. (2015). Postnatal maturation of GABAergic modulation of sensory inputs onto lateral amygdala principal neurons: development of sensory input inhibition in mouse lateral amygdala. J. Physiol. 593, 4387–4409. https://doi.org/10.1113/JP270645.

Bramen, J.E., Hranilovich, J.A., Dahl, R.E., Forbes, E.E., Chen, J., Toga, A.W., Dinov, I.D., Worthman, C.M., and Sowell, E.R. (2011). Puberty influences medial temporal lobe and cortical gray matter maturation differently in boys than girls matched for sexual maturity. Cereb. Cortex 21, 636–646. https://doi.org/10.1093/cercor/bhq137.

Breslau, J., Gilman, S.E., Stein, B.D., Ruder, T., Gmelin, T., and Miller, E. (2017). Sex differences in recent first-onset depression in an epidemiological sample of adolescents. Transl. Psychiatry 7, e1139. https://doi.org/10.1038/tp.2017.105.

Brinley-Reed, M., Mascagni, F., and McDonald, A.J. (1995). Synaptology of prefrontal cortical projections to the basolateral amygdala: an electron microscopic study in the rat. Neurosci.Lett. 202, 45–48. https://doi.org/10.1016/0304-3940(95)12212-5.

Cahill, L., Uncapher, M., Kilpatrick, L., Alkire, M.T., and Turner, J. (2004). Sex-Related hemispheric lateralization of amygdala function in emotionally influenced memory: an fMRI investigation. Learn. Mem. 11, 261–266. https://doi.org/10.1101/lm.70504.

Canli, T., Desmond, J.E., Zhao, Z., and Gabrieli, J.D.E. (2002). Sex differences in the neural basis of emotional memories. Proc. Natl. Acad. Sci. U S A 99, 10789–10794. https://doi.org/10.1073/pnas.162356599.

Casey, B.J., Jones, R.M., and Hare, T.A. (2008). The adolescent brain. Ann. N. Y. Acad. Sci. 1124, 111–126. https://doi.org/10.1196/annals.1440.010.

Chaouloff, F., Hémar, A., and Manzoni, O. (2007). Acute stress facilitates hippocampal CA1 metabotropic glutamate receptor-dependent long-term depression. J. Neurosci. 27, 7130–7135. https://doi.org/10.1523/JNEUROSCI.1150-07.2007.

Chavis, P., and Westbrook, G. (2001). Integrins mediate functional pre- and postsynaptic maturation at a hippocampal synapse. Nature 411, 317–321. https://doi.org/10.1038/35077101.

Chen, J.C.T., and Lang, E.J. (2003). Inhibitory control of rat lateral amygdaloid projection cells. Neuroscience 121, 155–166. https://doi.org/10.1016/S0306-4522(03)00430-5.

Christiansen, D.M., and Berke, E.T. (2020). Gender- and sex-based contributors to sex differences in PTSD. Curr.Psychiatry Rep. 22, 19. https://doi.org/10.1007/s11920-020-1140-y.

Dalpian, F., Rasia-Filho, A.A., and Calcagnotto, M.E. (2019). Sexual dimorphism, estrous cycle and laterality determine the intrinsic and synaptic properties of medial amygdala neurons in rat. J. Cell Sci. 132, jcs227793. https://doi.org/10.1242/jcs.227793.

Dalton, G.L., Wu, D.C., Wang, Y.T., Floresco, S.B., and Phillips, A.G. (2012). NMDA GluN2A and GluN2B receptors play separate roles in the induction of LTP and LTD in the amygdala and in the acquisition and extinction of conditioned fear. Neuropharmacology, Post-Traumatic Stress Disord. 62, 797–806. https://doi.org/10.1016/j.neuropharm.2011.09.001.

Damborsky, J.C., and Winzer-Serhan, U.H. (2012). Effects of sex and chronic neonatal nicotine treatment on NKCC1, KCC2, BDNF, NR2A and NR2B mRNA expression in the postnatal rat hippocampus. Neuroscience 225, 105–117. https://doi.org/10.1016/j.neuroscience.2012.09.002.

Danielewicz, J., and Hess, G. (2014). Early life stress alters synaptic modification range in the rat lateral amygdala. Behav. Brain Res. 265, 32–37. https://doi.org/10.1016/j.bbr.2014.02.012.

Daviu, N., Bruchas, M.R., Moghaddam, B., Sandi, C., and Beyeler, A. (2019). Neurobiological links between stress and anxiety. Neurobiol.Stress 11, 100191. https://doi.org/10.1016/j.ynstr.2019.100191.

Debanne, D., and Poo, M.-M. (2010). Spike-timing dependent plasticity beyond synapse - pre- and post-synaptic plasticity of intrinsic neuronal excitability. Front. Synaptic Neurosci. 2, 21. https://doi.org/10.3389/fnsyn.2010.00021.

Ehrlich, D.E., Ryan, S.J., Hazra, R., Guo, J.-D., and Rainnie, D.G. (2013). Postnatal maturation of GABAergic transmission in the rat basolateral amygdala. J. Neurophysiol. 110, 926–941. https://doi.org/10.1152/jn.01105.2012.

Ehrlich, D.E., Ryan, S.J., and Rainnie, D.G. (2012). Postnatal development of electrophysiological properties of principal neurons in the rat basolateral amygdala: development of principal neuron electrophysiology in the rat basolateral amygdala. J. Physiol. 590, 4819–4838. https://doi.org/10.1113/jphysiol.2012.237453.

Faber, E.S.L., Callister, R.J., and Sah, P. (2001). Morphological and electrophysiological properties of principal neurons in the rat lateral amygdala in vitro. J. Neurophysiol. 85, 714–723. https://doi.org/10.1152/jn.2001.85.2.714.

Faber, E.S.L., and Sah, P. (2002). Physiological role of calcium-activated potassium currents in the rat lateral amygdala. J. Neurosci. 22, 1618–1628. https://doi.org/10.1523/JNEUROSCI.22-05-01618.2002.

Farb, C., Aoki, C., Milner, T., Kaneko, T., and LeDoux, J. (1992). Glutamate immunoreactive terminals in the lateral amygdaloid nucleus: a possible substrate for emotional memory. Brain Res. 593, 145–158. https://doi.org/10.1016/0006-8993(92)91303-V.

Gall, C.M., Le, A.A., and Lynch, G. (2021). Sex differences in synaptic plasticity underlying learning. J. Neurosci. Res. 0, 1–19. https://doi.org/10.1002/jnr.24844.

Geary, C.G., Wilk, V.C., Barton, K.L., Jefferson, P.O., Binder, T., Bhutani, V., Baker, C.L., Fernando-Peiris, A.J., Mousley, A.L., Rozental, S.F.A., et al. (2021). Sex differences in gut microbiota modulation of aversive conditioning, open field activity, and basolateral amygdala dendritic spine density. J. Neurosci. Res. 99, 1780–1801. https://doi.org/10.1002/jnr.24848.

Goddings, A.-L., Mills, K.L., Clasen, L.S., Giedd, J.N., Viner, R.M., and Blakemore, S.-J. (2014). The influence of puberty on subcortical brain development. NeuroImage 88, 242–251. https://doi.org/10.1016/j.neuroimage.2013.09.073.

Greiner, E.M., Müller, I., Norris, M.R., Ng, K.H., and Sangha, S. (2019). Sex differences in fear regulation and reward-seeking behaviors in a fear-safety-reward discrimination task. Behav. Brain Res. 368, 111903. https://doi.org/10.1016/j.bbr.2019.111903.

Gruene, T.M., Flick, K., Stefano, A., Shea, S.D., and Shansky, R.M. (2015). Sexually divergent expression of active and passive conditioned fear responses in rats. eLife 4, e11352. https://doi.org/10.7554/eLife.11352.

Guadagno, A., Verlezza, S., Long, H., Wong, T.P., and Walker, C.-D. (2020). It is all in the right amygdala: increased synaptic plasticity and perineuronal nets in male, but not female, juvenile rat pups after exposure to early-life stress. J. Neurosci. 40, 8276–8291. https://doi.org/10.1523/JNEUROSCI.1029-20.2020.

Guo, Y., Liu, S., Cui, G.-B., Ma, L., Feng, B., Xing, J., Yang, Q., Li, X., Wu, Y., Xiong, L., et al. (2012).

Acute stress induces down-regulation of large-conductance Ca2+-activated potassium channels in the lateral amygdala. J. Physiol. 590, 875–886. https://doi.org/10.1113/jphysiol.2011.223784.

Hetzel, A., and Rosenkranz, J.A. (2014). Distinct effects of repeated restraint stress on basolateral amygdala neuronal membrane properties in resilient adolescent and adult rats. Neuropsychopharmacology 39, 2114–2130. https://doi.org/10.1038/npp.2014.60.

Huang, C.-C., Chen, J.-P., Yeh, C.-M., and Hsu, K.-S. (2012). Sex difference in stress-induced enhancement of hippocampal CA1 long-term depression during puberty. Hippocampus 22, 1622–1634. https://doi.org/10.1002/hipo.21003.

Hunsberger, M.S., and Mynlieff, M. (2020). BK potassium currents contribute differently to action potential waveform and firing rate as rat hippocampal neurons mature in the first postnatal week. J. Neurophysiol. 124, 703–714. https://doi.org/10.1152/jn.00711.2019.

Hwang, E.-K., and Lupica, C.R. (2020). Altered corticolimbic control of the nucleus accumbens by long-term Δ9-tetrahydrocannabinol exposure. Biol. Psychiatry 87, 619–631. https://doi.org/10.1016/j.biopsych.2019.07.024.

Iafrati, J., Malvache, A., Gonzalez Campo, C., Orejarena, M.J., Lassalle, O., Bouamrane, L., and Chavis, P. (2016). Multivariate synaptic and behavioral profiling reveals new developmental endophenotypes in the prefrontal cortex. Sci. Rep. 6, 35504. https://doi.org/10.1038/srep35504.

Janak, P.H., and Tye, K.M. (2015). From circuits to behaviour in the amygdala. Nature 517, 284–292. https://doi.org/10.1038/nature14188.

Kasanetz, F., and Manzoni, O.J. (2009). Maturation of excitatory synaptic transmission of the rat nucleus accumbens from juvenile to adult. J. Neurophysiol. 101, 2516–2527. https://doi.org/10.1152/jn.91039.2008.

Kirshner, H., Aguet, F., Sage, D., and Unser, M. (2013). 3-D PSF fitting for fluorescence microscopy: implementation and localization application. J. Microsc. 249, 13–25. https://doi.org/10.1111/j.1365-2818.2012.03675.x.

Krężel, W., Dupont, S., Krust, A., Chambon, P., and Chapman, P.F. (2001). Increased anxiety and synaptic plasticity in estrogen receptor β-deficient mice. Proc. Natl. Acad. Sci. U S A 98, 12278–12282. https://doi.org/10.1073/pnas.221451898.

Kuehner, C. (2017). Why is depression more common among women than among men? Lancet Psychiatry 4, 146–158. https://doi.org/10.1016/S2215-0366(16)30263-2.

Labouesse, M.A., Lassalle, O., Richetto, J., Iafrati, J., Weber-Stadlbauer, U., Notter, T., Gschwind, T., Pujadas, L., Soriano, E., Reichelt, A.C., et al. (2017). Hypervulnerability of the adolescent prefrontal cortex to nutritional stress via reelin deficiency. Mol. Psychiatry 22, 961–971. https://doi.org/10.1038/mp.2016.193.

Lê, S., Josse, J., and Husson, F. (2008). FactoMineR: an R package for multivariate analysis. J. Stat. Softw. 25, 1–18. https://doi.org/10.18637/jss.v025.i01.

Lebron-Milad, K., and Milad, M.R. (2012). Sex differences, gonadal hormones and the fear extinction network: implications for anxiety disorders. Biol. Mood Anxiety Disord. *2*, 3. https://doi.org/10.1186/2045-5380-2-3.

Mahan, A.L., and Ressler, K.J. (2012). Fear conditioning, synaptic plasticity and the amygdala: implications for posttraumatic stress disorder. Trends Neurosci.Spec. Issue Neuropsychiatr.Disord. *35*, 24–35. https://doi.org/10.1016/j.tins.2011.06.007.

Malenka, R.C., and Bear, M.F. (2004). LTP and LTD: an embarrassment of riches. Neuron *44*, 5–21. https://doi.org/10.1016/j.neuron.2004.09.012.

Malinow, R., and Malenka, R.C. (2002). AMPA receptor trafficking and synaptic plasticity. Annu. Rev. Neurosci. *25*, 103–126. https://doi.org/10.1146/annurev.neuro.25.112701.142758.

Manduca, A., Bara, A., Larrieu, T., Lassalle, O., Joffre, C., Layé, S., and Manzoni, O.J. (2017). Amplification of mGlu5-endocannabinoid signaling rescues behavioral and synaptic deficits in a mouse model of adolescent and adult dietary polyunsaturated fatty acid imbalance. J. Neurosci. *37*, 6851–6868. https://doi.org/10.1523/JNEUROSCI.3516-16.2017.

Martin, H.G.S., Lassalle, O., Brown, J.T., and Manzoni, O.J. (2016). Age-dependent long-term potentiation deficits in the prefrontal cortex of the Fmr1 knockout mouse model of fragile X syndrome. Cereb. Cortex *26*, 2084–2092. https://doi.org/10.1093/cercor/bhv031.

Martin, H.G.S., and Manzoni, O. (2014). Late onset deficits in synaptic plasticity in the valproic acid rat model of autism. Front. Cell.Neurosci. *8*, 23. https://doi.org/10.3389/fncel.2014.00023.

Matos, H.Y., Hernandez-Pineda, D., Charpentier, C.M., Rusk, A., Corbin, J.G., and Jones, K.S. (2020). Sex differences in biophysical signatures across molecularly defined medial amygdala neuronal subpopulations. eNeuro *7*. ENEURO.0035-20. https://doi.org/10.1523/ENEURO.0035-20.2020.

McLean, C.P., Asnaani, A., Litz, B.T., and Hofmann, S.G. (2011). Gender differences in anxiety disorders: prevalence, course of illness, comorbidity and burden of illness. J. Psychiatr. Res. *45*, 1027–1035. https://doi.org/10.1016/j.jpsychires.2011.03.006.

Mierau, S.B., Meredith, R.M., Upton, A.L., and Paulsen, O. (2004). Dissociation of experience-dependent and -independent changes in excitatory synaptic transmission during development of barrel cortex. Proc. Natl. Acad. Sci. U S A *101*, 15518–15523. https://doi.org/10.1073/pnas.0402916101.

Moyer, C.E., and Zuo, Y. (2018). Cortical dendritic spine development and plasticity: insights from in vivo imaging. Curr.Opin.Neurobiol.Developmental Neurosci. *53*, 76–82. https://doi.org/10.1016/j.conb.2018.06.002.

Mozhui, K., Karlsson, R.-M., Kash, T.L., Ihne, J., Norcross, M., Patel, S., Farrell, M.R., Hill, E.E., Graybeal, C., Martin, K.P., et al. (2010). Strain differences in stress responsivity are associated with divergent amygdala gene expression and

glutamate-mediated neuronal excitability. J. Neurosci. *30*, 5357–5367. https://doi.org/10.1523/JNEUROSCI.5017-09.2010.

Nestler, E.J., Barrot, M., DiLeone, R.J., Eisch, A.J., Gold, S.J., and Monteggia, L.M. (2002). Neurobiology of depression. Neuron *34*, 13–25. https://doi.org/10.1016/S0896-6273(02)00653-0.

Paoletti, P., Bellone, C., and Zhou, Q. (2013). NMDA receptor subunit diversity: impact on receptor properties, synaptic plasticity and disease. Nat. Rev. Neurosci. *14*, 383–400. https://doi.org/10.1038/nrn3504.

Pape, H.-C., and Pare, D. (2010). Plastic synaptic networks of the amygdala for the acquisition, expression, and extinction of conditioned fear. Physiol. Rev. *90*, 419–463. https://doi.org/10.1152/physrev.00037.2009.

Phelps, E.A. (2004). Human emotion and memory: interactions of the amygdala and hippocampal complex. Curr.Opin.Neurobiol. *14*, 198–202. https://doi.org/10.1016/j.conb.2004.03.015.

Picard, N., Takesian, A.E., Fagiolini, M., and Hensch, T.K. (2019). NMDA 2A receptors in parvalbumin cells mediate sex-specific rapid ketamine response on cortical activity. Mol. Psychiatry *24*, 828–838. https://doi.org/10.1038/s41380-018-0341-9.

Power, J.M., and Sah, P. (2008). Competition between calcium-activated K+ channels determines cholinergic action on firing properties of basolateral amygdala projection neurons. J. Neurosci. *28*, 3209–3220. https://doi.org/10.1523/JNEUROSCI.4310-07.2008.

Proaño, S.B., and Meitzen, J. (2020). Estradiol decreases medium spiny neuron excitability in female rat nucleus accumbens core. J. Neurophysiol. *123*, 2465–2475. https://doi.org/10.1152/jn.00210.2020.

Proaño, S.B., Morris, H.J., Kunz, L.M., Dorris, D.M., and Meitzen, J. (2018). Estrous cycle-induced sex differences in medium spiny neuron excitatory synaptic transmission and intrinsic excitability in adult rat nucleus accumbens core. J. Neurophysiol. *120*, 1356–1373. https://doi.org/10.1152/jn.00263.2018.

Przybysz, K.R., Gamble, M.E., and Diaz, M.R. (2021). Moderate adolescent chronic intermittent ethanol exposure sex-dependently disrupts synaptic transmission and kappa opioid receptor function in the basolateral amygdala of adult rats. Neuropharmacology *188*, 108512. https://doi.org/10.1016/j.neuropharm.2021.108512.

Qi, X., Zhang, K., Xu, T., Yamaki, V.N., Wei, Z., Huang, M., Rose, G.M., and Cai, X. (2016). Sex differences in long-term potentiation at temporoammonic-CA1 synapses: potential implications for memory consolidation. PLoS ONE *11*, e0165891. https://doi.org/10.1371/journal.pone.0165891.

Radley, J.J., Farb, C.R., He, Y., Janssen, W.G.M., Rodrigues, S.M., Johnson, L.R., Hof, P.R., LeDoux, J.E., and Morrison, J.H. (2007). Distribution of NMDA and AMPA receptor subunits at thalamo-amygdaloid dendritic spines. Brain Res. *1134*, 87–94. https://doi.org/10.1016/j.brainres.2006.11.045.

Rammes, G., Eder, M., Dodt, H.-U., Kochs, E., and Zieglgänsberger, W. (2001). Long-term depression in the basolateral amygdala of the mouse involves the activation of interneurons. Neuroscience *107*, 85–97. https://doi.org/10.1016/S0306-4522(01)00336-0.

Rau, A.R., Chappell, A.M., Butler, T.R., Ariwodola, O.J., and Weiner, J.L. (2015). Increased basolateral amygdala pyramidal cell excitability may contribute to the anxiogenic phenotype induced by chronic early-life stress. J. Neurosci. *35*, 9730–9740. https://doi.org/10.1523/JNEUROSCI.0384-15.2015.

Rosenkranz, J.A., Venheim, E.R., and Padival, M. (2010). Chronic stress causes amygdala hyperexcitability in rodents. Biol. Psychiatry Amygdala Activity Anxiety: Stress Effects *67*, 1128–1136. https://doi.org/10.1016/j.biopsych.2010.02.008.

Rouzer, S.K., and Diaz, M.R. (2021). Factors of sex and age dictate the regulation of GABAergic activity by corticotropin-releasing factor receptor 1 in the medial sub-nucleus of the central amygdala. Neuropharmacology *189*, 108530. https://doi.org/10.1016/j.neuropharm.2021.108530.

Ryan, S.J., Ehrlich, D.E., and Rainnie, D.G. (2016). Morphology and dendritic maturation of developing principal neurons in the rat basolateral amygdala. Brain Struct.Funct. *221*, 839–854. https://doi.org/10.1007/s00429-014-0939-x.

Sage, D., Donati, L., Soulez, F., Fortun, D., Schmit, G., Seitz, A., Guiet, R., Vonesch, C., and Unser, M. (2017). DeconvolutionLab2: an open-source software for deconvolution microscopy. Methods *115*, 28–41. https://doi.org/10.1016/j.ymeth.2016.12.015.

Sah, P., and Louise Faber, E.S. (2002). Channels underlying neuronal calcium-activated potassium currents. Prog.Neurobiol. *66*, 345–353. https://doi.org/10.1016/S0301-0082(02)00004-7.

Scherf, K.S., Smyth, J.M., and Delgado, M.R. (2013). The amygdala: an agent of change in adolescent neural networks. Horm.Behav. Puberty Adolescence *64*, 298–313. https://doi.org/10.1016/j.yhbeh.2013.05.011.

Scheyer, A.F., Borsoi, M., Pelissier-Alicot, A.-L., and Manzoni, O.J.J. (2020a). Maternal exposure to the cannabinoid agonist win 55,12,2 during lactation induces lasting behavioral and synaptic alterations in the rat adult offspring of both sexes. eNeuro *7*. ENEURO.0144-20. https://doi.org/10.1523/ENEURO.0144-20.2020.

Scheyer, A.F., Borsoi, M., Pelissier-Alicot, A.-L., and Manzoni, O.J.J. (2020b). Perinatal THC exposure via lactation induces lasting alterations to social behavior and prefrontal cortex function in rats at adulthood. Neuropsychopharmacol. Off. Publ. Am. Coll. Neuropsychopharmacol. *45*, 1826–1833. https://doi.org/10.1038/s41386-020-0716-x.

Scheyer, A.F., Borsoi, M., Wager-Miller, J., Pelissier-Alicot, A.-L., Murphy, M.N., Mackie, K., and Manzoni, O.J.J. (2019). Cannabinoid exposure via lactation in rats disrupts perinatal programming of the GABA trajectory and select early-life behaviors. Biol. Psychiatry *87*, 666–677. https://doi.org/10.1016/j.biopsych.2019.08.023.

Schneider, M. (2013). Adolescence as a vulnerable period to alter rodent behavior. Cell Tissue Res 354, 99–106. https://doi.org/10.1007/s00441-013-1581-2.

Selleck, R.A., Zhang, W., Samberg, H.D., Padival, M., and Rosenkranz, J.A. (2018). Limited prefrontal cortical regulation over the basolateral amygdala in adolescent rats. Sci. Rep. 8, 17171. https://doi.org/10.1038/s41598-018-35649-0.

Shansky, R.M., and Murphy, A.Z. (2021). Considering sex as a biological variable will require a global shift in science culture. Nat. Neurosci. 24, 457–464. https://doi.org/10.1038/s41593-021-00806-8.

Spear, L.P. (2000). The adolescent brain and age-related behavioral manifestations. Neurosci.Biobehav. Rev. 24, 417–463. https://doi.org/10.1016/S0149-7634(00)00014-2.

Thomazeau, A., Lassalle, O., Iafrati, J., Souchet, B., Guedj, F., Janel, N., Chavis, P., Delabar, J., and Manzoni, O.J. (2014). Prefrontal deficits in a murine model overexpressing the down syndrome candidate gene dyrk1a. J. Neurosci.

Off. J. Soc. Neurosci. 34, 1138–1147. https://doi.org/10.1523/JNEUROSCI.2852-13.2014.

van den Buuse, M., Low, J.K., Kwek, P., Martin, S., and Gogos, A. (2017). Selective enhancement of NMDA receptor-mediated locomotor hyperactivity by male sex hormones in mice. Psychopharmacology (Berl.) 234, 2727–2735. https://doi.org/10.1007/s00213-017-4668-8.

Wang, S.-J., and Gean, P.-W. (1999). Long-term depression of excitatory synaptic transmission in the rat amygdala. J. Neurosci. 19, 10656–10663. https://doi.org/10.1523/JNEUROSCI.19-24-10656.1999.

Wang, W., Le, A.A., Hou, B., Lauterborn, J.C., Cox, C.D., Levin, E.R., Lynch, G., and Gall, C.M. (2018). Memory-Related synaptic plasticity is sexually dimorphic in rodent Hippocampus. J. Neurosci. 38, 7935–7951. https://doi.org/10.1523/JNEUROSCI.0801-18.2018.

Washburn, M., and Moises, H. (1992). Electrophysiological and morphological properties of rat basolateral amygdaloid neurons in vitro. J. Neurosci. 12, 4066–4079. https://doi.org/10.1523/JNEUROSCI.12-10-04066.1992.

Yang, R., Zhang, B., Chen, T., Zhang, S., and Chen, L. (2017). Postpartum estrogen withdrawal impairs GABAergic inhibition and LTD induction in basolateral amygdala complex via down-regulation of GPR30. Eur. Neuropsychopharmacol. 27, 759–772. https://doi.org/10.1016/j.euroneuro.2017.05.010.

Zhang, J.-Y., Liu, T.-H., He, Y., Pan, H.-Q., Zhang, W.-H., Yin, X.-P., Tian, X.-L., Li, B.-M., Wang, X.-D., Holmes, A., et al. (2019). Chronic stress remodels synapses in an amygdala circuit–specific manner. Biol. Psychiatry 85, 189–201. https://doi.org/10.1016/j.biopsych.2018.06.019.

Zhang, W., and Rosenkranz, J.A. (2012). Repeated restraint stress increases basolateral amygdala neuronal activity in an age-dependent manner. Neuroscience 226, 459–474. https://doi.org/10.1016/j.neuroscience.2012.08.051.

Zhang, Y., Garcia, E., Sack, A.-S., and Snutch, T.P. (2020). L-type calcium channel contributions to intrinsic excitability and synaptic activity during basolateral amygdala postnatal development. J. Neurophysiol. 123, 1216–1235. https://doi.org/10.1152/jn.00606.2019.

STAR★METHODS

KEY RESOURCE TABLE

REAGENT or RESOURCE	SOURCE	IDENTIFIER
Experimental models: Organisms/strains		
Rat: Wistar	Janvier Labs	N/A
Software and algorithms		
GraphPad Prism v9	GraphPad	RRID:SCR_002798
R Project for Statistical Computing 3.6.1	R Foundation	RRID:SCR_001905
Fiji	NIH	RRID:SCR_002285
Imaris	Bitplane	RRID:SCR_007370

RESOURCE AVAILABILITY

Lead contact

Further information and requests for resources should be directed to and will be fulfilled by the lead contact, Olivier J. Manzoni (olivier.manzoni@inserm.fr).

Materials availability

This study did not generate unique reagents.

Data and code availability

All data reported in this paper will be shared by the lead contact upon request. This paper does not report original code. Any additional information required to reanalyze the data reported in this paper is available from the lead contact upon request.

EXPERIMENTAL MODEL AND SUBJECT DETAILS

Animals were treated in compliance with the European Communities Council Directive (86/609/EEC) and the United States NIH Guide for the Care and Use of Laboratory Animals. The French Ethical committee authorized the project APAFIS#26537–2020070812023339. All rats were obtained from Janvier Labs and group-housed (two to four rats per cage) with *ad libitum* access to food and water. All groups represent data from a minimum of 2 litters. The animal housing room was maintained on a 12 h-day light/dark cycle at constant room temperature (20 ± 1°C) and humidity (60%). Data were collected blind to the estrous cycle unless specified. Female and male rats were classified based on the timing of their pubertal maturation. Male and female rats do not reach puberty at the same time (Schneider, 2013). Thus, the female ages groups were Pubescent 33 <p< 38 and Adult at 90 <p< 120. Male groups were: Pubescent 41 <p< 56 and Adult at 90 <p< 120 (Figure S1A). All animals were experimentally naive and used only once.

METHOD DETAILS

Electrophysiology

Male and female rats were anesthetized with isoflurane and killed as previously described (Bara et al., 2018; Borsoi et al., 2019; Scheyer et al., 2019, 2020a, 2020b). The brain was sliced (300 μm) in the coronal plane with a vibratome (Integraslice, Campden Instruments) in a sucrose-based solution at 4 °C (in mM as follows: 87 NaCl, 75 sucrose, 25 glucose, 2.5 KCl, four $MgCl_2$, 0.5 $CaCl_2$, 23 $NaHCO_3$ and 1.25 NaH_2PO_4). Immediately after cutting, slices containing the basolateral amygdala (BLA) were stored for 1h at 32 °C in a low-calcium ACSF that contained (in mm) as follows: 130 NaCl, 11 glucose, 2.5 KCl, 2.4 $MgCl_2$, 1.2 $CaCl_2$, 23 $NaHCO_3$, 1.2 NaH_2PO_4, and were equilibrated with 95% O_2/5% CO_2 and then held at room temperature until the time of recording.

During the recording, slices were placed in the recording chamber and superfused at 2 mL/min with normal ACSF that contained (in mM): 130 NaCl, 11 glucose, 2.5 KCl, 2.4 MgCl$_2$, 2.4 CaCl$_2$, 23 NaHCO$_3$, 1.2 NaH$_2$PO$_4$, equilibrated with 95% O$_2$/5% CO$_2$. All experiments were done at 32 °C. The superfusion medium contained picrotoxin (100 μM, Sigma) to block GABA-A receptors, except for low frequency stimulation (LFS) experiments. All drugs were added at the final concentration to the superfusion medium. Field and whole-cell patch-clamp recordings were performed with an Axopatch-200B amplifier, data were low pass filtered at 2kHz, digitized (10 kHz, DigiData 1440A, Axon Instrument), collected using Clampex 10.2 and analyzed using Clampfit 10.2 (all from Molecular Device, Sunnyvale, USA).

Whole-cell patch-clamp of visualized BLA principal neurons and field potential recordings were made as previously described (Bara et al., 2018; Borsoi et al., 2019; Scheyer et al., 2019, 2020a, 2020b) in coronal slices containing the BLA. Neurons were visualized using an upright microscope with infrared illumination. The intracellular solution was based on K$^+$ gluconate (in mM: 145 K$^+$ gluconate, three NaCl, one MgCl$_2$, one EGTA, 0.3 CaCl$_2$, two Na$_2$ATP, and 0.3 NaGTP, 0.2 cAMP, buffered with 10 HEPES). The pH was adjusted to 7.2 and osmolarity to 290–300 mOsm. Electrode resistance was 2–4 MOhms. Access resistance compensation was not used, and acceptable access resistance was <30 MOhms. The potential reference of the amplifier was adjusted to zero prior to breaking into the cell. Current-voltage (I-V) curves were made by a series of hyperpolarizing to depolarizing 50 pA current steps after breaking into the cell. To determine rheobase and action potential properties a series of depolarizing 10 pA current steps was applied. Membrane resistance was estimated from the I–V curve around resting membrane potential (Bara et al., 2018; Borsoi et al., 2019; Scheyer et al., 2019, 2020a, 2020b). Spontaneous EPSCs (sEPSCs) were recorded at −70mV for at least 10 min as previously described (Kasanetz and Manzoni, 2009; Martin et al., 2016). To determine AMPA/NMDA ratios, the intracellular solution was based on cesium methanesulfonate (CsMe, mM): 143 CsMeSO$_3$, five NaCl, one MgCl$_2$, one EGTA, 0.3 CaCl$_2$, 10 HEPES, two Na$_2$ATP, 0.3 NaGTP and 0.2 cAMP (pH 7.3 and 290–300 mOsm). AMPA/NMDA ratios were calculated by measuring evoked EPSCs (having AMPAR and NMDAR components) at +30 mV. The AMPAR component was isolated by bath application of an NMDAR antagonist (APV; 50 μM, Tocris)(Kasanetz and Manzoni, 2009).

For extracellular field potential recordings, the stimulating electrode was positioned in the lateral amygdala (LA), close to the external capsule (EC), dorsolateral to the recording electrode placed into the adjacent BA (Figure S1B). The glutamatergic nature of the field EPSP (fEPSP) was systematically confirmed at the end of the experiments using the ionotropic glutamate receptor antagonist CNQX (20 μM), which specifically blocked the synaptic component without altering the non-synaptic component. Both fEPSP area and amplitude were analyzed. Stimulation was performed with a glass electrode filled with ACSF and the stimulus intensity was adjusted ∼60% of maximal intensity after performing an input-output curve. For LTP experiments, baseline stimulation frequency was set at 0.1 Hz and plasticity was induced by a theta burst stimulation (TBS; five trains of four pulses at 100 Hz, 200 ms train interval, repeated 4 times at 10 s interval). For LTD experiments, baseline stimulation frequency was set at 0.0666 Hz and plasticity was induced by low frequency stimulation (LFS; 900 pulses at 1 Hz).

Electrophysiological data analysis

Action potential properties were determined from the first spike induced during current clamp experiment. The voltage at which point the dV/dt trace first passed 5 mV/ms was the threshold. fAHP was measured at a local minimum directly following spike's repolarization within a couple of ms. The mAHP was measured at a local minimum distinct from the fAHP and occurring 15–150 ms after the spike. The frequency and amplitude of sEPSCs were analyzed with Axograph X using a double exponential template: f(t) = exp(-t/rise) + exp(-t/decay) (rise = 0.5 ms and decay = 3 ms). The detection threshold for the events was set at 2.5 times the baseline noise SD For AMPA/NMDA ratios, NMDAR component was obtained by digital subtraction of the AMPA-EPSC from the dual component EPSC (AMPA/NMDA ratio = peak AMPA-EPSC at +30mV/peak NMDA-EPSC at +30 mV). For field recording experiments, the magnitude of plasticity was calculated at 30–40 min after induction as percentage of baseline responses. Percent of LTP, referred to as LTP (%) = -1x(fEPSP amplitude at baseline (in % of baseline) - fEPSP amplitude at 30–40min (in % of baseline)). Percent of LTD, referred to as LTD (%) = fEPSP amplitude at baseline (in % of baseline) - fEPSP amplitude at 30–40min (in % of baseline). The percent of LTD or LTP was calculated and cumulative frequency distribution plots were built for each group (Chaouloff et al., 2007; Martin and Manzoni, 2014).

Dendritic spines reconstruction and analysis

All neurons recorded with CsMe solution were also loaded with neurobiotin through patch pipettes. Slices were then fixed overnight in 4% paraformaldehyde, rinsed with PBS and incubated overnight at 4 °C with streptavidin-AlexaFluor555 (1:200 in PBS). Slices were mounted for subsequent confocal imaging. All filled neurons corresponded to typical glutamatergic BLA neurons (Washburn and Moises, 1992) (e.g., large cell body, spiny dendrites, pyramidal to stellate shape). Only neurons showing proper filling of the dendritic tree were included in the analysis. Five to eleven dendrites per neuron were analyzed. Dendrites were located approximately at 70 to 140 μm of the soma. Stack images were acquired using a Zeiss LSM-800 confocal microscope equipped with a 40 oil-immersion objective (NA: 1,4). Frame size was of 512 × 512 pixels with a ×4 zoom. Laser power and photomultiplier gain were adjusted to obtain few pixels with maximum intensity on dendrite shaft and the offset range was tuned to cutoff background noise. Tri-dimensional deconvolution of each stack was performed with Fiji software to compensate the spherical aberration and to correct the z-smear for reliable spine morphology. Point-spread function (PSF) were computed using PSFGenerator plugging (Kirshner et al., 2013) and deconvolution was realized with DeconvolutionLab2 plugin (Sage et al., 2017) using the Richardson-Lucy method. Tri-dimensional reconstruction and semiautomated analysis were performed with Imaris (Bitplane, Zurich, Switzerland).

QUANTIFICATION AND STATISTICAL ANALYSIS

With the exception of Principal Component Analysis (PCA, see below), statistical analysis of data was performed with Prism (GraphPad Software) using tests indicated in figure legends after outlier subtraction (Grubb's test, alpha level 0.05). In summary, intrinsic and action potential's properties, after hyperpolarization potentials, maximum input-output, mean frequency and amplitude of sEPSCs, AMPA/NMDA ratio and dendritic spine density were analyzed with two-way ANOVA followed by Šídák multiple comparison tests (main factors of 2-way ANOVAs were sex and developmental stage). Morphological parameters of dendritic spines were analyzed with a non-parametric test because of the complex distribution of the data, i.e., Kruskal-Wallis test followed by Dunn's multiple comparisons tests. Pre versus post analysis of LTP and LTD data were analyzed with paired t-test.

Considering the numerous parameters reported in the evaluation of intrinsic and action potential properties, PCA was computed using FactoMineR package (Lê et al., 2008) with R (RCore Team (2020). R: A language and environment for statistical computing. R Foundation for Statistical Computing, Vienna, Austria.URL https://www.R-project.org/.).

p values < 0.05 were considered statistically significant. n meaning and exact value, as well as represented precision measures, are described in figure legends.